Lawrence Berkeley Laboratory
UNIVERSITY OF CALIFORNIA

Accelerator & Fusion Research Division

Presented at the 1st Joint US/CERN School on Particle Accelerator Nonlinear Dynamics, Santa Margherita di Pula, Sardinia, Italy, January 31-February 5, 1985; and to be published in the Proceedings

NONLINEAR DYNAMICS: A PERSONAL PERSPECTIVE

L.J. Laslett

December 1984

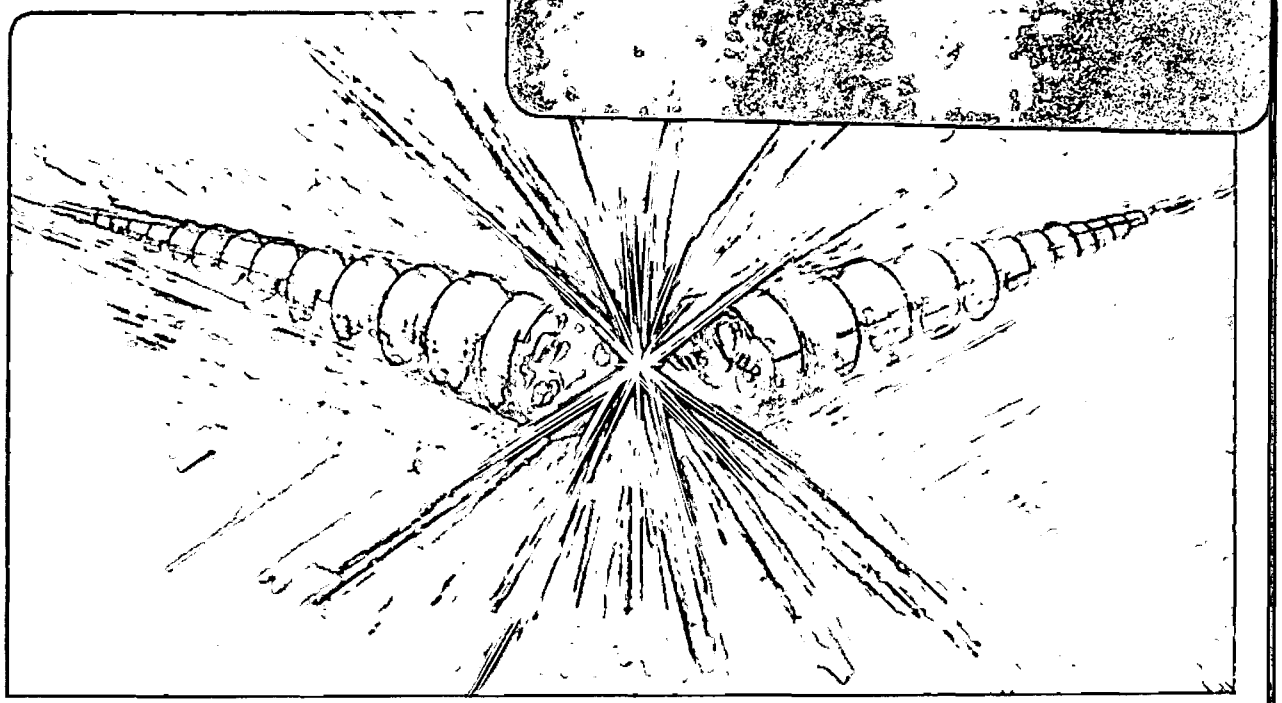

Prepared for the U.S. Department of Energy under Contract DE-AC03-76SF00098

DISCLAIMER

LBL-18987 Rev.

NONLINEAR DYNAMICS
A PERSONAL PERSPECTIVE*

L. Jackson Laslett

Lawrence Berkeley Laboratory
University of California
Berkeley, California 94720

December 1984

* This work was supported by the Office of Energy Research, Office of Basic Energy Sciences, Department of Energy under Contract No. DE-AC03-76SF00098.

NONLINEAR DYNAMICS
A PERSONAL PERSPECTIVE*

L. Jackson Laslett
Lawrence Berkeley Laboratory
University of California
Berkeley, California 94720

INTRODUCTION AND OUTLINE

The earlier talks in this Conference have given us a welcome insight into the phenomena that I shall call collectively by the term stochasticity. It is good to see the attention that this field now is receiving, since I have had the feeling that for many years it was rather unfashionable in the West. The increasing availability of digital computers during the last few decades certainly has assisted in providing illustrative examples that serve to spread an awareness of the characteristics of these phenomena, but we should not overlook that many of the basic features and concepts were appreciated by early workers such as Poincaré, Maxwell,[1]† and the elder Birkhoff.

I was asked to present a "Personal Perspective" relating to work in this field, which might be interpreted as an invitation to mention historical instances in which, of my personal knowledge, the evolution of accelerator technology led to accelerator designers developing certain specific issues related to possible stochastic behavior. The phenomena encountered in studying such issues have a very captivating intrinsic interest; with the increasing availability of personal computers and interactive terminals, some may wish to review such issues or to pursue related issues partly for enlightenment but also partly for fun.

In this connection, a few comments or caviats may be in order:

(1) For execution of some problems, a high-precision capability may be essential, but

(2) There are some issues that (as we shall see) can be illustrated quite usefully with the aid of no more than a simple desk calculator;

(3) An interactive graphic capability can be exceedingly convenient, and revealing ("serendipity");

(4) Algebraic transformations can be more convenient to study than the evolution of solutions to differential equations, and yet provide equally valid illustrations of significant phenomena, but

(5) If one wishes to examine solutions to differential equations, adoption of a "Hamiltonian" or "canonical" integration algorithm would be reassuring. Such an algorithm has been presented, as a

*This work was supported by the Office of Energy Research, Office of Basic Energy Sciences, Department of Energy under Contract No. DE-AC03-76SF00098.

†References are given at the end of the this Introduction (p. 2).

3^{rd}-order algorithm, by R. Ruth,[2] and it is understood that Dr. Ruth has since developed a similar 4^{th}-order integration algorithm -- at least for equations derivable from a Hamiltonian function of the form $H = f(\vec{p}) + V(\vec{q}, t)$.

With integration procedures of more conventional type (e.g., for Runge-Kutta algorithms), features such as conservation of phase-space area are not precisely maintained for Hamiltonian systems, and one must guard against the development of significant consistent spurious damping of phase-space area in extended runs. One may reasonably presume that physical systems of interest to us may differ, perhaps inadvertently, from those postulated for our computations but that, nonetheless, the physical systems in fact will be canonical.

The phenomena we have heard discussed in these recent sessions of our Conference of course have their implications in fields that extend far beyond the dynamics of particles in accelerators and storage rings. The field of astronomy certainly presents situations of obvious interest in this regard. To move outside of fields of physical science, it is noteworthy that quite simple and reasonable models for the annual change of populations of prey and predator can lead to astonishing oscillatory or erratic variations of the representative populations.[3] I suspect that similar effects might be seen in economic models. The sensitivity of behavior with respect to details of even quite simple models, as we have begun to recognize in some of our own work, surely should lead model makers to view their results with less than complete assurance.

Issues I hope to discuss are:[4]

Development of Stochasticity from Area-Preserving Transformations;

Limiting (Resonant) Frequencies for Particle Motion in the Median Plane of a Strong-Focusing Ring -- Examples;

Bifurcation.

REFERENCES AND NOTES

1. See quotation from Maxwell, given on p. 111 of M. V. Berry's very informative article in the A.I.P. Conference Proceedings, No. 46 (1978).
2. Proc. 1983 Particle Accelerator Conf., IEEE Trans. Nucl. Sci. NS-30 (No. 4), pp. 2669-2671.
3. See, for example, Review Articles by Robert M. May, Nature (London) 261, 459-467 (10 June 1976); 269, 471-477 (6 October 1977).
4. Similar discussions of some of these issues have been given earlier in Proc. 1974 Internat. Conf. High Energy Accelerators, pp. 394-401 (Stanford, California; 1974) and A.I.P. Conference Proceedings, No. 46 (Siebe Jorna, Ed.), pp. 221-247 (Amer. Inst. Physics, N.Y.; 1978).

I. CANONICAL TRANSFORMATIONS

The direct use of canonical transformations can be convenient for the investigation and illustration of trajectory behavior in particle accelerators or storage rings ("tracking studies"). McMillan has proposed[1] a convenient form for a transformation, that we shall generalize to several degrees of freedom, and is such that

(1) it is canonical,

(2) it is readily obtained from a transformation for which there is a simple particle-optics interpretation, and

(3) it exhibits interesting (and useful) symmetries.

One may start by considering a linear homogeneous transformation followed by a thin-lens abrupt non-linear change of slope (or "momentum"):

$$\left.\begin{aligned} Q_i' &= a_i Q_i + b_i P_i \\ P_i' &= c_i Q_i + d_i P_i + F_i(Q_1', Q_2', \ldots) \end{aligned}\right\} , \tag{1}$$

wherein primes denote iterates. We require that

$$\begin{vmatrix} a_i & b_i \\ c_i & d_i \end{vmatrix} = 1 \tag{1a}$$

and

$$\frac{\partial F_i}{\partial Q_j'} = \frac{\partial F_j}{\partial Q_i'} \tag{1b}$$

[so that, if one wishes, one may write $F_i = -\frac{\partial}{\partial Q_i'} V(Q_1', Q_2', \ldots)$] in order that the transformation be canonical. [In numerical work with transformations such as (1), it is desirable that the coefficients a_1, b_1, etc., and coefficients entering into the functions F_i in multi-dimensional cases, be so selected and employed that the above conditions for canonical behavior are satisfied exactly. Small errors in the specification of such constants can result in a troublesome progressive and consistent failure of solutions to satisfy conservation theorems (such as those that pertain to phase-space areas or volume).]

One may now rewrite the transformation (1) in terms of other variables, introducing

$$\left.\begin{aligned} x_i &= b_i^{-1/2} Q_i \\ y_i &= a_i b_i^{-1/2} Q_i + b_i^{1/2} P_i \end{aligned}\right\} \tag{2}$$

to obtain

$$\left.\begin{aligned} x_i' &= y_i \\ y_i' &= -x_i + f_i(y_1, y_2, \ldots) \end{aligned}\right\}, \tag{3}$$

where $$f_i(y_1, y_2, \ldots) = (a_i + d_i) y_i + b_i^{1/2} F_i(b_1^{1/2} y_1, b_2^{1/2} y_2, \ldots) \tag{3a}$$

and wherein we require [in multi-dimensional cases, in correspondence to Eqn. (1b)] that

$$\frac{\partial f_i}{\partial y_j} = \frac{\partial f_j}{\partial y_i} \quad . \tag{3b}$$

The transformation (3) is in the McMillan form, generalized to permit its application in cases that involve more than a single conjugate pair of variables.[2]

As an area-preserving transformation for a single pair of canonical variables, the McMillan transformation (3) has several interesting and potentially helpful simple characteristics:[1]

(1) Geometrically, an application of the transformation can be represented on the x,y diagram by a reflection about the principal diagonal followed by a vertical reflection (parallel to the y axis) about the curve y = 1/2 f(x).

(2) If two points are iteratively related, by one application of the transformation, such points mirrored about the principal diagonal also are iteratively related (in the inverse order).

(3) If two points are iteratively related, by one application of the transformation, such points mirrored vertically about the curve y = 1/2 f(x) also are iteratively related (in the inverse order).

(4) Order-1 fixed point(s) lie on the intersection of the curve y = 1/2 f(x) with the principal diagonal y = x.

(5) If the function $f(\eta) = \Phi(\eta) + \Phi^{-1}(\eta)$, where Φ^{-1} denotes the <u>inverse</u> function, then curves $y = \Phi(x)$ and $x = \Phi(y)$ each constitute invariant curves (intersecting at order-1 fixed points). When such

curves completely enclose an area of the phase plane, phase points of course then are unable to move into or out from such an area as a result of applications of the transformation (although erratic motion nonetheless may develop within the area) -- see Fig. I.1.[4]

It is interesting that several area-preserving transformations of which use has been made in the past can be put into McMillan's form (3) by means of some simple (sometimes linear) change of variables. We list some examples of this equivalence in Note 5 at the end of this Chapter.

It can be informative to employ a simple algebraic transformation to illustrate a mechanism for the development of stochasticity. It is convenient for this purpose to consider a quadratically nonlinear transformation proposed by de-Vogelaere and rewritten in McMillan's form (with $f(y) = 2y^2$):

$$\left.\begin{aligned} x' &= y \\ y' &= -x + 2y^2 \end{aligned}\right\} . \qquad (4)$$

This transformation possesses a stable order-1 fixed point at the origin and an unstable (hyberbolic) order-1 fixed point at 1, 1 -- as illustrated in Fig. I.2 by intersections of the curve $y=1/2\ f(x) = x^2$ with the principal diagonal. The motion of points in the immediate neighborhood of the unstable fixed point is governed by the tangential-mapping transformation evaluated at that point. This local linearization leads to eigenvector directions $dy/dx = 2 \pm \sqrt{3}$ along which points will move directly away from or directly toward the fixed point, with distances from the fixed point then changing by the respective factors $\lambda = 2 \pm \sqrt{3}$ per iteration.

It is now instructive to depict, as on Fig. I.2, the evolutionary track followed by line segments originating with these slopes close to the unstable fixed point and extended by repeated applications of the transformation or its inverse. A line segment such as GFE thus transforms to a segment EDC as a result of one application of the forward transformation, and the points CDE likewise lead to points EFG under the application of the inverse transformation. The line segments that in this way are extended from the fixed point, by repeated application of this transformation and of its inverse, do <u>not</u>, however, intersect smoothly (e.g., at points such as D on Fig. I.2) and thus result in the formation of the "loops" designated by L on Fig. I.2. Such loops are all of equal area, as a result of the area-preservation and diagonal symmetry of the transformation. Accordingly, as a line segment such as GFE is advanced by repeated applications of the forward transformation, it will develop loops that become increasingly elongated as their intersection points (such as points C, B, and A) approach the fixed point with a closer and closer spacing.

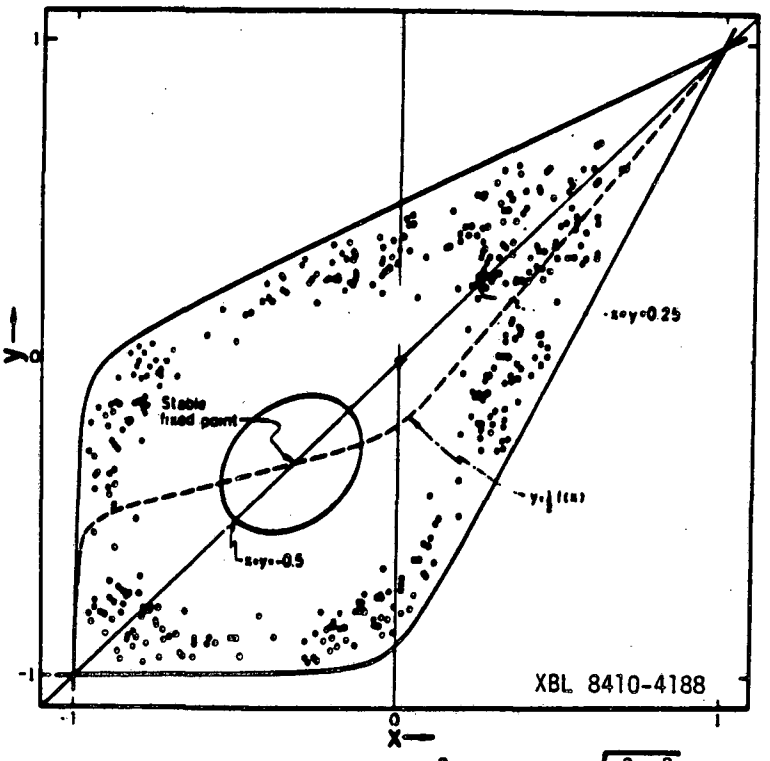

Fig. I.1. The case $f(x) = (3x-1)/2 \pm k^2/2(x+1) + \sqrt{x^2+k^2}$, with 0.1 as the value of k. The invariant boundary consists of two hyperbolas. The results of two computer runs are shown. A run starting at x = y = -0.5 generates the apparently smooth curve surrounding the stable fixed point at x = y ≈ -0.328, and a run starting at x = y = 0.25 gives, for the first 400 iterations, the scattered points indicated as dots.

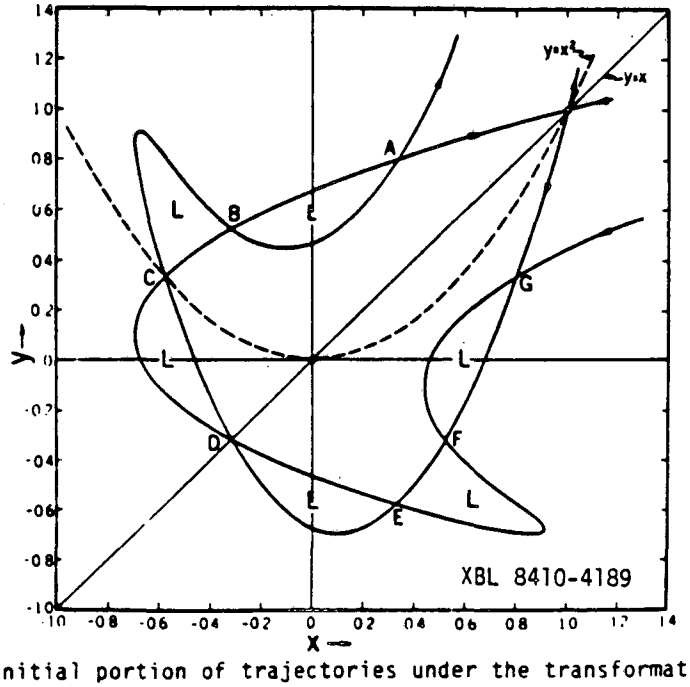

Fig. I.2 Initial portion of trajectories under the transformation $x' = y$, $y' = -x+2y^2$, leading away from (or toward) the unstable fixed point at x = 1, y = 1. The arrows indicate the directions in which points are moved by the transformation. The point pairs AG, BF, CE illustrate the first symmetry, the point pairs AE, BD the second symmetry. The areas of the loops marked L are all equal.

As a result of these loops developing into "worms" that are progressively narrower and more elongated, the phase-plane diagram can rapidly develop a great complexity (Fig. I.3) and repeated applications of the transformation to a phase point situated in this region will lead to a "stochastic" or apparently irregular scatter of its iterates. The region affected by such stochastic behavior need not, however, extend fully into the "interior" of the diagram. Thus, smooth closed phase trajectories may exist in this example at small amplitudes, as is suggested by some simple curves drawn near the origin on Fig. I.3. [These latter curves are characterized by a distinctive four-pointed shape as a result of the phase advance per iteration for this transformation approaching $2\pi/4$ as the amplitude approaches zero.]

Similar stochastic behavior of course can originate in association with unstable fixed points of higher order. Fig. I.4 illustrates such features of the Hénon-Froeschlé mapping[5b,7] (with $\cos \alpha = 0.22$), re-expressed in the McMillan form. Additional details of this example have been shown in Refs.[10] (Figures on p. 399) and[11] (Figures on pp.342 and 343).

Synchrotron motion, although frequently described by means of simple nonlinear differential equations, is most appropriately described by means of a <u>transformation</u> that recognizes the impulsive character of the forces applied at discrete cavity locations. The construction of a Hamiltonian function for such a problem thus strictly requires the inclusion of δ-functions or similar location-dependent functions to specify the localization of these forces and the Hamiltonian will <u>not</u> constitute a constant of the motion.

A transformation to describe synchrotron motion for a coasting beam may be written, in the form of the "standard mapping",[5c,8] as

$$\left.\begin{aligned} y' &= y - K \sin \pi x \\ x' &= x + ky' \end{aligned}\right\}, \tag{5}$$

wherein

- y = Fractional departure of energy from the reference value at the entrance to the cavity,
- πx = electrical phase angle of field relative to the particle,
- K $\propto$ applied voltage, and
- k $\propto$ derivative of revolution period with respect to energy.

To obtain a convenient symmetry in the phase plots, it is useful to introduce the variables $X = x$ and $Y = y - (K/2) \sin \pi x$, thereby measuring energy departures at mid-passage through the cavities. One accordingly then employs the transformation

$$\left.\begin{aligned} X' &= X + k\,[\, Y - (K/2) \sin \pi X \,] \\ Y' &= Y - (K/2)\,[\, \sin \pi X + \sin \pi X' \,] \end{aligned}\right\} \tag{6}$$

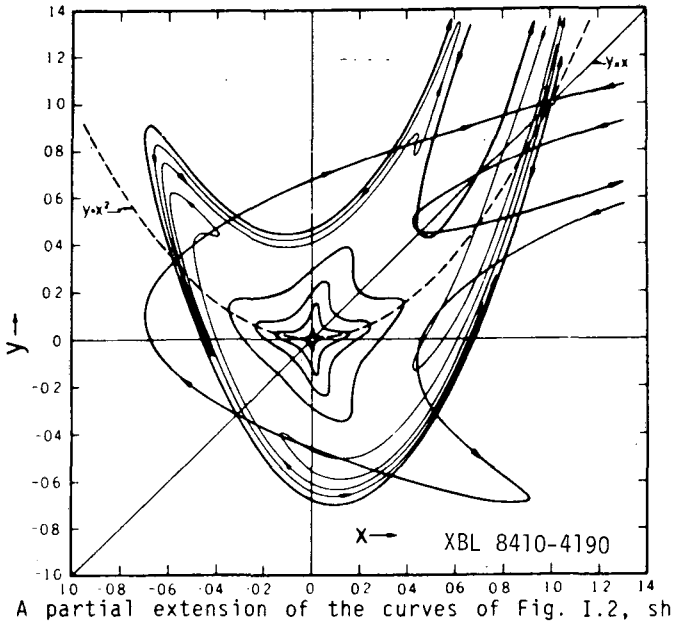

Fig. I.3 A partial extension of the curves of Fig. I.2, showing "tentacles" reaching off the figure and "worms" in the interior. Since the entrance channel for the "worms" becomes very narrow, the figure becomes difficult to draw completely as the iteration progresses. Some apparently closed curves around the stable fixed point at x = 0, y = 0 are also shown. The peculiar behavior near the orgin seems less mysterious if one recalls that the function y = 1/2f(x) approaches the limit of zero slope, where the curve degenerates to four points, and where the slightest perturbation can cause a slow migration about the center and a concomitant slow change in radius.

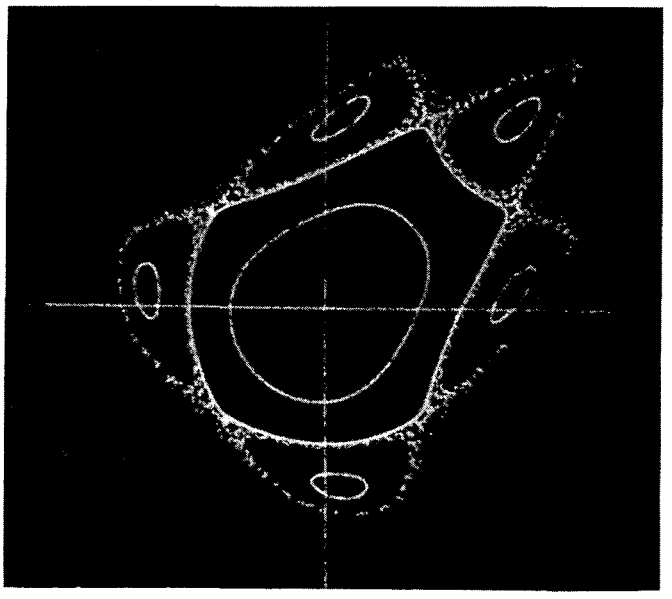

Fig. I.4. Apparently smooth phase curves and a scattering of points resulting from iteration of the Hénon-Froeschlé transformation, with cos α = 0.22 and coordinates x,y appropriate to expressing the transformation in the McMillan form. Five islands of stability (containing stable fixed points of order 5) are seen surrounding the area associated with the order-1 fixed point at the orgin. The outermost smooth curve, shown as bounding this inner area, resulted from the starting values X_o = 0.5350, Y_o = 0 (Froeschlé notation), and the scattered points result from X_o = 0.5375, Y_o = 0. Scale (as indicated by the coordinate axes): -1.0 to 1.0. XBB 840-7763

and plots Y vs. X modulo 2. A stable first-order fixed point occurs at X = 0, Y = 0; other similar fixed points, that correspond to harmonic operation, occur at X = 0 and Y equal to any integer multiple of 2/k.

For K and k small, the phase advance of small-amplitude synchrotron oscillations from one cavity transit to the next is approximately $\sigma_s = \sqrt{\pi K k}$ radian and substantially-smooth separatrices appear to extend between unstable fixed points at X = ±1 to enclose stable "bucket areas" of half height $\delta Y \cong 2\sqrt{K/\pi k}$ -- see Fig. I.5, plotted for K = 0.1π and k = 0.1, wherein one also sees depicted indications of sub-harmonic trajectories in the region between the major buckets shown at Y = 0 and at Y = 20. The ratio of bucket height to the separation of major buckets thus may be measured by $\frac{2}{\pi}\sigma_s$ and will be small when the phase advance σ_s is small.

For substantially larger values of K (or of k), corresponding to values of σ_s very much greater than normally employed in accelerator operation, bucket heights may become comparable with the separation between major buckets. The development of stochasticity, especially in the neighborhood of the unstable fixed points at X = ±1, then becomes very pronounced -- see Fig. I.6, plotted for K = 0.8π and with k = 0.1 (as before). In the case to which Fig. I.5 applies (K = 0.1π, k = 0.1), however, the development of stochasticity is so subtle that it can be demonstrated computationally only with considerable care and it results in the formation of loops whose estimated individual areas are a fraction only ~ 1/(5 x 10^{11}) of the full area of a major bucket [result reported in unpublished 1960 Lawrence Berkeley Laboratory Report ERAN-57 and cited in A.I.P. Proceedings No. 46, p. 226 (1978)[11]].

An algebraic transformation may be employed as a means of obtaining an approximate representation of solutions to differential equations. As an example, we may note a transformation cited earlier [5d,9].

$$\left.\begin{aligned} X' &= AX + (1-A^2)Y + (1-A)[\,X + (1-A)Y\,]^2 \\ Y' &= -X + AY + [\,X + (1-A)Y\,]^2 \end{aligned}\right\} , \qquad (7)$$

that was originally introduced in the expectation that it would depict approximately the median-plane motion of charged particles in a spiral-sector accelerator. First-order fixed points occur at the origin (0,0) and at (1,0). With the parameter A assigned the value A = -5/8, the fixed point at the origin is stable (small-amplitude tune, $\sigma_0 = \cos^{-1} A \cong 128.68$ deg., or approximately 0.35745 times 2π radian), while the point at (1,0) is unstable. The region considered to be of interest for accelerator operation was the roughly triangular region enclosed by the apparent separatrices that connect the third-order unstable fixed points F_1, F_2, F_3 shown on Figs. I.7 and I.8 (and for which the area approaches zero if the small-amplitude tune approaches 2π/3).

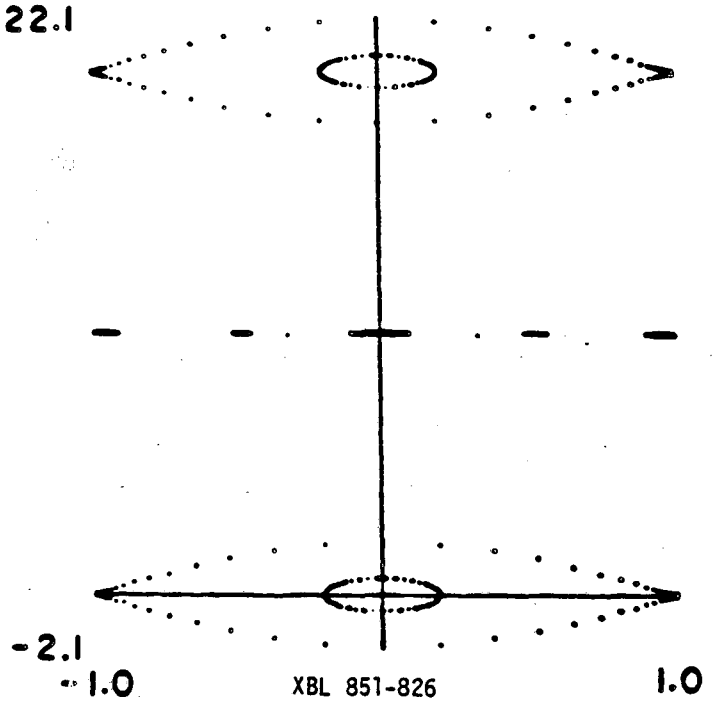

Fig. I.5 X,Y phase plot for a coasting beam under the influence of an R.F. cavity with $K/\pi = 0.1$, $k = 0.1$ -- as computed by Eqs. (6). Y is plotted mod. 2.

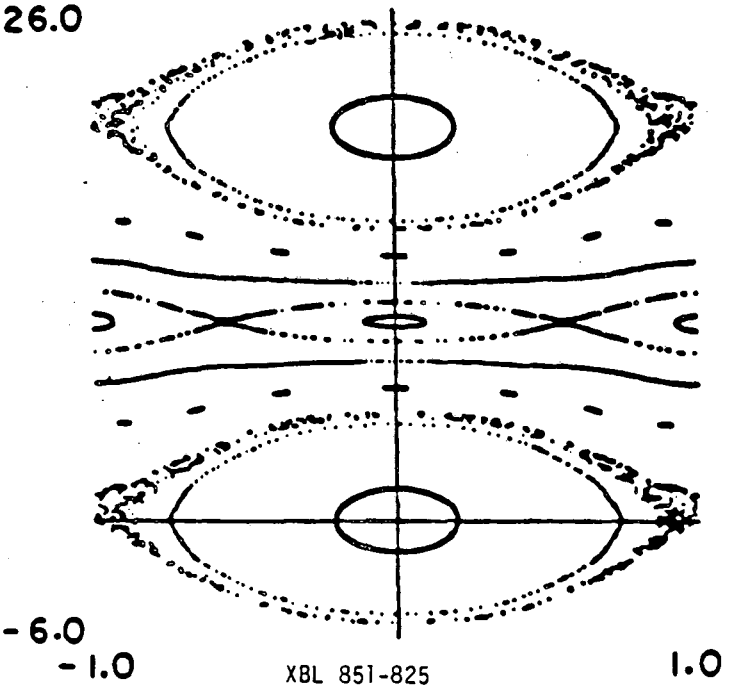

Fig. I.6 Phase plot similar to Fig. I.5, but for operation with $K/\pi = 0.8$, showing the obvious development of complex structure.

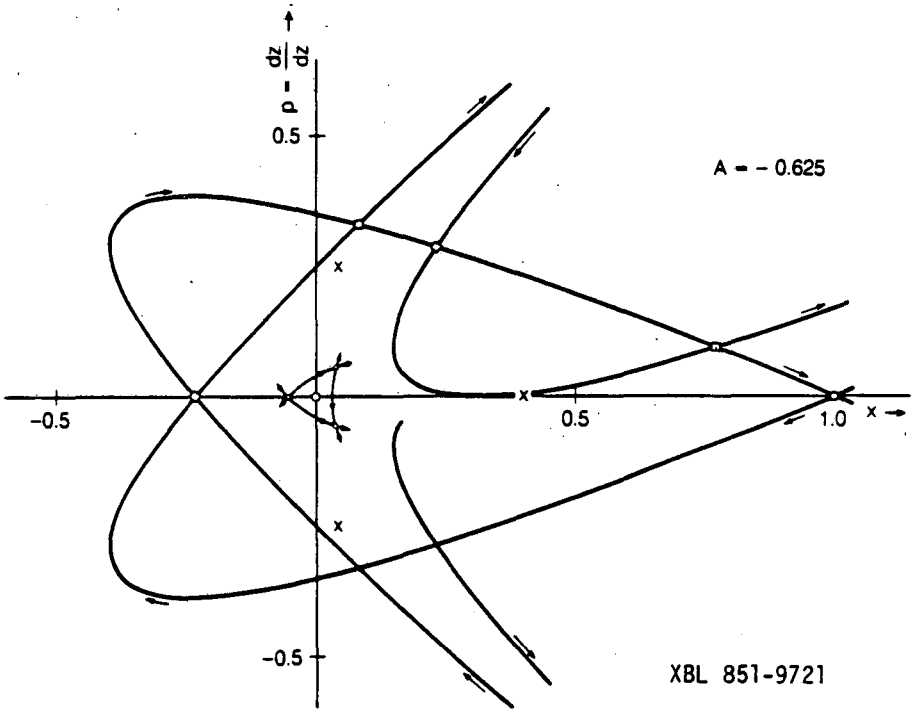

Fig. I.7 Phase diagram for the area-preserving transformation (7) with A = -5/8. Large loops are seen to develop from eigenvector directions extended from the first-order unstable fixed point situated at (1,0). Points denoted by squares (⊡) are related by the transformation, as are also points denoted by diamonds (◇). Our interest will be confined primarily, however, to the roughly triangular area sketched near the third-order unstable fixed points F_1, F_2, F_3 shown by small circles near the center of the diagram. Points denoted by crosses (X) are third-order fixed points that are strongly unstable <u>with reflection</u>.

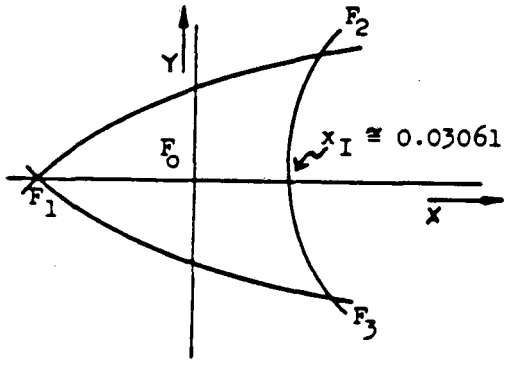

Sketch for $A = -5/8$

$\cos^{-1}A \cong (0.35745)(2\pi)$

Area $\cong 5.5 \times 10^{-3}$
(would shrink to zero
if $A \to -1/2$)

$$F_1: \left(-\frac{\sqrt{41}-5}{26}, 0\right) = (-0.053966\cdots, 0)$$

$$F_{2,3}: \left(\frac{1}{26}, \pm\frac{4\sqrt{41}-16}{169}\right) = (0.03846\cdots, \pm 0.05688\cdots)$$

XBL 851-824

Fig. I.8. Detail of Fig. 7, showing the apparently stable area bounded by the third-order fixed points F_1, F_2, F_3. [Transformation (7), with A = -5/8.]

It then was of interest to inquire whether these curves can be demonstrated to be imperfect separatrices and, if so, to investigate the extent to which the resulting stochasticity permeates into the interior. Eigenvector directions extended toward the x-axis from the fixed points F_2, F_3, were found,[6] upon careful examination, not to intersect smoothly. The areas of the loops so generated constituted, however, only a very small fraction (*circa* $1/10^8$) of the area F_1 F_2 F_3 and no evidence was found to indicate stochasticity within any significant portion of the region of interest.

REFERENCES AND NOTES

1. Edwin M. McMillan, "A Problem in the Stability of Periodic Systems," *in* "Topics in Modern Physics--A Tribute to Edward V. Condon," pp. 219-244 (Colorado Assoc. University Press, Boulder, Colorado; 1971).

2. McMillian's original work,[1] pertaining to a single pair of working variables, introduced the change of variables

$$\left.\begin{aligned} x &= Q \\ y &= aQ + bP \end{aligned}\right\}$$

(a "scaling" transformation, for which the Jacobian although constant is not necessarily equal to unity) to obtain his form

$$\left.\begin{aligned} x' &= y \\ y' &= -x + f(y) \end{aligned}\right\},$$

with $f(y) = (a + d)y + bF(y)$. The phase advance σ per iteration of y *vs.* x oscillatory motion is given, for small amplitude motion by $\cos \sigma = 1/2 \left.\frac{df(y)}{dy}\right|_{y=0}$ and, if F(y) is restricted to terms of order higher than the first, $\cos \sigma = (a + d)/2$. The canonical character of the transformation (3) given in the text can be verified through evaluation of the fundamental Poisson bracket expressions or, alternatively, by rewriting the equations (3) in the form

$$\left.\begin{aligned} x_i &= -y_i' + f_i(y_1, y_2, \ldots) \\ &= -y_i' - \partial V(y_1, y_2, \ldots)/\partial y_i \\ x_i' &= y_i \end{aligned}\right\}$$

and noting that such equations are derivable from a generating function

$$G(y_1, y_2, \ldots; y_1', y_2', \ldots) = V(y_1, y_2, \ldots) + \sum_i y_i y_i'$$

by application of the relations

$$\left.\begin{aligned} x_i &= -\,\partial G/\partial y_i \\ x_i' &= +\,\partial G/\partial y_i' \end{aligned}\right\} \quad .$$

As a multi-dimensional illustration of a transformation of the form (1) introduced in the text, we may refer to a form that (with a change of notation, including interchange of "old" with "new" variables) was employed by Meier and Symon[3] in a study of coupling resonances:

$$\left.\begin{aligned} Q_1' &= (\cos\sigma_1)Q_1 + (\sin\sigma_1)P_1 \\ P_1' &= (-\sin\sigma_1)Q_1 + (\cos\sigma_1)P_1 - \frac{k}{2}(Q_2')^2 \\ Q_2' &= (\cos\sigma_2)Q_2 + (\sin\sigma_2)P_2 \\ P_2' &= (-\sin\sigma_2)Q_2 + (\cos\sigma_2)P_2 - kQ_1'Q_2' \end{aligned}\right\} \quad .$$

This transformation is seen to be of the form (1) with $V(Q_1', Q_2') = (k/2)Q_1'(Q_2')^2$.

3. H. Meier and K. R. Symon, Proc. 1959 Internat. Conf. on High-Energy Accelerators, p. 253-262 (C.E.R.N., Geneva; 1959).

4. Figure I.1 has been presented by McMillan as Fig. 8 of Ref. (1). The transformation illustrated is for $f(x) = (1/2)(3x - 1) - (1/2)k^2/(x + 1) + \sqrt{x^2 + k^2}$ with 0.1 as the value of k. This function is expressible as $f(x) = \Phi(x) + \Phi^{-1}(x)$, with $\Phi(x) = x - 1 + \sqrt{x^2 + k^2}$ and $\Phi^{-1}(x) = (1/2)(x + 1) - (1/2)k^2/(x + 1)$. The curves $y = \Phi(x)$ and $y = \Phi^{-1}(x)$ are shown as boundary curves passing through the two order-1 unstable fixed points. The erratic distribution of points that fall within a portion of the region interior to this boundary originated from $x_0 = y_0 = 0.25$. McMillan has also shown, and illustrated by Figs. 4-7 of Ref.(1), that a function of the form $f(x) = -(Bx^2 + Dx)/(Ax^2 + Bx + C)$ employed in his area-preserving transformation will lead to the phase plane being covered by nested invariant curves of the form

$$Ax^2y^2 + B(x^2y + xy^2) + C(x^2 + y^2) + D\,xy = \text{const.}$$

5. We list here several area-preserving transformations that can be put into McMillan's form by means of a suitable change of variables.

   a.) The DeVogelaere Transformation (generalized, cf Refs. 1 and 6):

$$X' = Y + F(X), \qquad Y' = -X + F(X') \quad .$$

With introduction of variables such that

$$\left.\begin{aligned} X &= x \\ Y &= y - F(x) \end{aligned}\right\},$$

the transformation assumes the area-preserving McMillan form with $f(y) = 2\,F(y)$.

b.) A Transformation of Hénon and Froeschlé:[7]

$$\left.\begin{aligned} X' &= X\cos\alpha - (Y - X^2)\sin\alpha \\ Y' &= X\sin\alpha + (Y - X^2)\cos\alpha \end{aligned}\right\}.$$

With introduction of variables x,y such that

$$\left.\begin{aligned} X &= (\sin\alpha)^{1/2}\, y \\ Y &= (\sin\alpha)^{-1/2}\,(x - y\cos\alpha) \end{aligned}\right\} \text{(a linear transformation)},$$

the transformation assumes the area-preserving McMillan form with $f(y) = 2(\cos\alpha)y + (\sin\alpha)^{3/2}\, y^2$.

c.) A "Generalized Standard Mapping":[8]

$$\left.\begin{aligned} I' &= I + g(\Theta) \\ \Theta' &= \Theta + I' \end{aligned}\right\}.$$

With the linear change of variables given by

$$\left.\begin{aligned} \Theta &= y \\ I &= y - x \end{aligned}\right\},$$

we obtain the area-preserving McMillan transformation with $F(y) = 2y + g(y)$.

d.) A transformation cited in Note 9:

$$\left.\begin{aligned} X' &= AX + (1 - A^2)Y + (1 - A)\,[\,X + (1 - A)Y\,]^2 \\ Y' &= -X + AY + [\,X + (1 - A)Y\,]^2 \end{aligned}\right\}.$$

We introduce variables x,y by a linear "scaling transformation" such that

$$\left.\begin{aligned} X &= \frac{1}{4}\,\frac{(1+A)^{3/4}}{(1-A)^{1/4}}\,(x+y) \\ Y &= \frac{1}{4}\,\frac{(1+A)^{3/4}}{(1-A)^{5/4}}\,(-x+y) \end{aligned}\right\}\ ,$$

For which the Jacobian has the value $\frac{1}{8}\left(\frac{1+A}{1-A}\right)^{3/2}$ to obtain the area-preserving

McMillan transformation with

$$f(y) = 2Ay + (1-A^2)^{3/4}\,y^2\ .$$

6. L. Jackson Laslett, Edwin M. McMillan, and Jürgen Moser, "Long-Term Stability for Particle Orbits," Courant Institute Report NYO-1480-101 (New York University, N.Y.; 1968).

7. M. Hénon, Q. Appl. Math. XXVII, 291-312 (1969). See also C. Froeschlé, Astron. and Astrophys. 9, 15-23 (1970).

8. A. Lichtenberg and M. A. Lieberman, "Regular and Stochastic Motion," p. 156 (Springer; 1983).

9. This transformation was employed in the expectation that it would depict the median-plane motion of charged particles in a spiral-sector FFAG accelerator operated near a third-integral resonance. Some properties of this transformation have been described and discussed in Ref. 6.

10. L. Jackson Laslett, Proc. 1974 Internat. Conf. High Energy Accelerators, pp. 394-401 (Stanford, California; 1974).

11. L. Jackson Laslett, A.I.P. Conference Proceedings, No. 46 (Siebe Jorna, Ed.), pp. 221-247 (Amer. Inst. Physics, N.Y.; 1978).

II. LIMITING (RESONANT) FREQUENCIES FOR PARTICLE MOTION IN THE MEDIAN PLANE

Erratic dynamical behavior can impose definite limits to the permissible amplitudes of individual-particle oscillations in alternating-gradient focusing systems when nonlinearities are present. Thus, the limiting amplitude for motion in the median plane of a strong focusing ring typically occurs in association with a system of fixed points in the phase plane, with a detectable stochasticity first making its appearance in the neighborhood of the unstable fixed points of the system.

Stochasticity in the phase plane for motion with a single spatial degree of freedom of course may be contained by the occurrence of a surrounding KAM (Kolmogorov-Arnol'd-Moser) closed curve, but regions of sufficient amplitude can be found wherein stochastic behavior will carry a phase point to markedly greater, and totally unacceptable, amplitudes. [An associated phenomenon is that of period-doubling bifurcation (to be illustrated in Chapter III), wherein a change of a parameter of a focusing system leads to a previously stable fixed-point system becoming unstable with reflection and to a new fixed-point system of double period becoming created. A sequence of such period-doubling bifurcations, occurring for smaller and smaller increments of the governing parameter, results in a bifurcation lattice or "tree" that may be claimed to terminate in "chaos".]

Informative illustrations of amplitude limitations for stable motion accordingly may be obtained by the examination of solutions to simple differential equations representative of median-plane motion in an idealized alternating-gradient ring. Examples of such equations, for which results are presented below, are

$$\frac{d^2x}{dZ^2} = - A\,(x + 1/8\,x^2)\cos Z \qquad (1)$$

and

$$\frac{d^2x}{dZ^2} = - A\,(x + 1/12\,x^3 + 1/384\,x^5)\cos Z, \qquad (2)$$

wherein the factor cos Z results in a alternating gradient focusing action with a period scaled to 2π. With appropriate scaling of the dependent variable, Eqn. (1) is intended to represent the effect of alternating sextupole fields (to supplement the quadrupole focusing), while Eqn. (2) represents x motion (suitably scaled) in a Maxwellian magnetic field for which the y component in the median plane is taken to be proportional to $I_2(x)/x$ prior to truncation.[1] It will be recognized that, for simplicity in constructing these equations, the obliquity of the trajectories has been neglected to the extent that the longitudinal component of velocity is treated as constant. Trajectories computed from such equations should be strictly area-preserving when plotted on a x, $x' = dx/dZ$ plane. Use of a canonical integration algorithm thus in principle would be preferable for such

computations, but application of a fourth-order Runge-Kutta-Gill algorithm with a suitably small step size has appeared also to be satisfactory for the present illustrative purposes.

The coefficient A that appears in Eqns. (1) and (2) serves to determine the "tune" (or the phase advance, σ_0, per period) for small-amplitude oscillations. For a fixed value of A that results in reasonable stable motion about the origin, the solutions to Eqn.(1) are found to exhibit tunes that decrease with increasing amplitude, while the tunes for solutions to Eqn. (2) become greater for large amplitude solutions. In either case, it is of interest to examine, for various values of σ_0, the extent to which the tune assumes a different value at the limit of stable motion and to attempt to identify the fixed-point system that appears to be associated with the onset of instability in such cases.[2] Such investigations are conveniently conducted by means of phase plots wherein values of x, x' for solutions to the equation of interest are plotted at one-period intervals -- e.g., for the present equations, at $Z = 0 \ \underline{\text{mod}}. \ 2\pi$.

With Eqn. (1), the symmetry is such that plots made at $Z=0 \ \underline{\text{mod}}. \ 2\pi$ (or, alternatively , at $Z = \pi \ \underline{\text{mod}}. \ 2\pi$) will exhibit a symmetry in x' about the x axis, and solutions to Eqn. (2) when so plotted will exhibit also a symmetry in x about the x' axis. In directing attention here to instabilities associated with motion confined to the x, Z plane, one, of course, must recognize that motion occurring in two transverse directions will be subject to additional limitations, perhaps of a different character (Arnol'd diffusion?), that well may merit investigation.

A.

$$\frac{d^2x}{dZ^2} = -A(x + 1/8\ x^2)\ \cos Z$$

Median-plane motion of the type of interest here is illustrated by Fig. II.1 for solutions to Eqn. (1) with A = 0.2736, for which the small-amplitude tune is such that $\sigma_0 \cong 74.59$ deg. One notes the appearance of a pronounced order 5/1 fixed-point system ($\sigma = 72$ deg.) at an intermediate amplitude. Some stochasticity indeed may be present in association with this system -- and, if so, might be demonstrable computationally with sufficient care -- but one sees that in any case this system is surrounded by an apparently smooth closed phase trajectory (launched at $x_0 = 1.55$, $x'_0 = 0$). At a somewhat larger amplitude, however, an order 16/3 system ($\sigma = 67.5$ deg.) becomes evident, for which some small loops may be seen on the Figure near the stable fixed points of this system, but for which it is more notable that stochasticity associated with the unstable fixed points develops to reveal a gross instability.

Figure II.2 illustrates the manner in which the computational runs portrayed in Fig. II.1 appear if plotted at the quarter-period points $Z = \pi/2 \ \underline{\text{mod}} \ 2\pi$. One

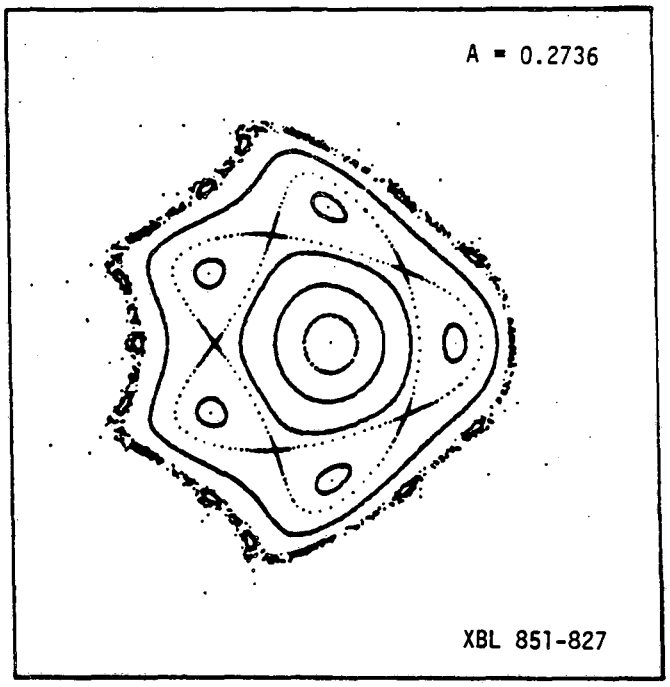

Fig. II.1 x' vs. x phase plot, at Z=0 mod.2π, for solutions to Eqn. (1) with A = 0.2736 ($\sigma_0 \cong 74.59$ deg.) to the scales:
Horizontal: -3.0 to 3.0, for x; Vertical: -0.3 to 0.3, for x'.
Instability is seen to arise from stochasticity associated with a fixed-point system of order 16/3 ($\sigma = 3 \times 360/16 = 67.5$ deg.). The apparently smooth phase trajectory situated somewhat inside this fixed-point system resulted from a computation launched at $x_0 = 1.55$, $x_0' = 0$.

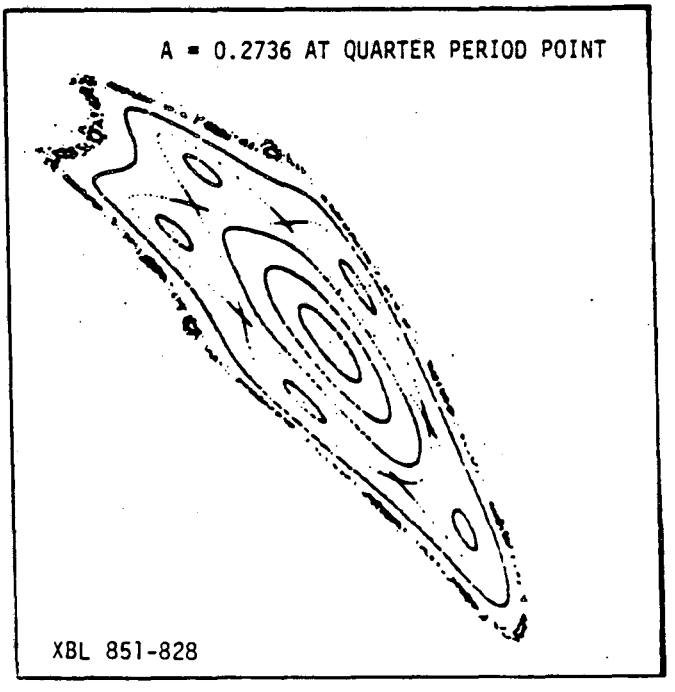

Fig. II.2 Phase plot for the runs of Fig. 1, plotted at Z = π/2 mod. 2π.
Scales: Horizontal: -2.0 to 2.0, for x; Vertical: -0.6 to 0.6, for x'.

expects maximum spatial excursions to occur near the centers of focusing regions, and phase plots constructed for Z = 0 mod. 2π accordingly seem most appropriate for the present work.

It is of interest to examine in a similar manner the character of solutions to Eqn. (1) for various values of the parameter A. Results are shown by a sequence of phase plots (Figs. II.3-II.8a) and are summarized in the following Table.

Parameter A	Small-Amplitude Tune, σ_0 (deg)	Estimated Range of x at Z=0 mod. 2π & Associated Tune (deg)	Nearby Fixed-Point System Order, & Tune(deg)
0.23	61.303277	-2.4 to 1.69 (~52.6 deg)	7/1, 1 X 360/7=51.4286
0.24	64.265071	-2.3 to 1.72 (~56.0 deg)	13/2, 2 X 360/13=55.3846
0.25	67.273942	-1.7 to 1.43 (~61.6 deg)	6/1, 1 X 360/6=60.
0.26	70.334408	-1.89 or ~ 1.9 to 1.61 (~62.8 deg)	23/4, 4 X 360/23=62.6087
0.26525	71.963493	-1.86 to 1.65 (~64.7 deg)	39/7, 7 X 360/39=64.6154 28/5, 5 X 360/28=64.2857
0.26670	72.416288	-1.82 to 1.57 (~65.9 deg)	11/2, 2 X 360/11=65.4545

In some instances the fixed-point system associated with the first onset of gross stochastic instability appears to be of a rather high order (and indeed in such cases may become more difficult to specify). It may be particularly notable that with variations of A covering a fairly small range in this sequence of cases, many distinctly different fixed-point systems appear to be associated in turn with the stability limit.

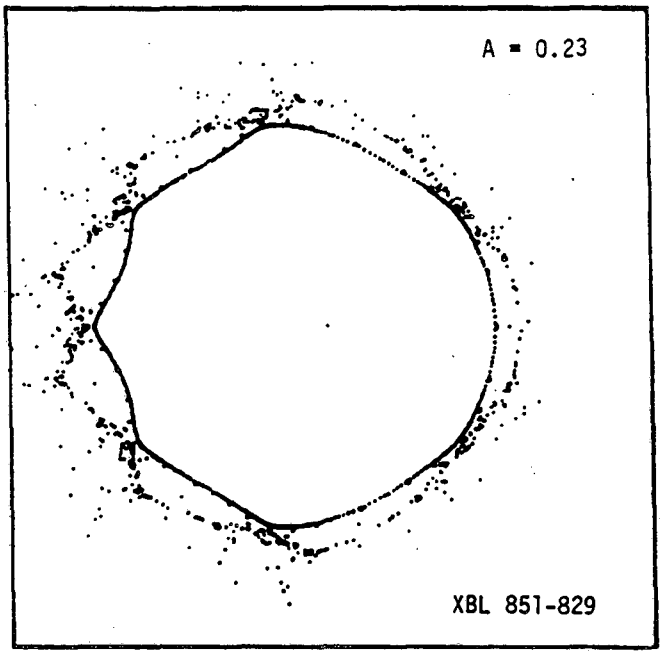

Fig. II.3 Phase plot for A = 0.23; Scales:
Horizontal: -3.25 to 3.25 for x; Vertical: -0.30 to 0.30, for x'.
Shown are an apparently limiting phase trajectory (launched with $x_0 = -2.4$, $x_0' = 0$), a sequence of order 7/1 stable fixed points, and an erratic run resulting from a launch substantially at an order 7/1 unstable fixed point (taken to be at approximately $x_0 = -2.465$, $x_0' = 0$).

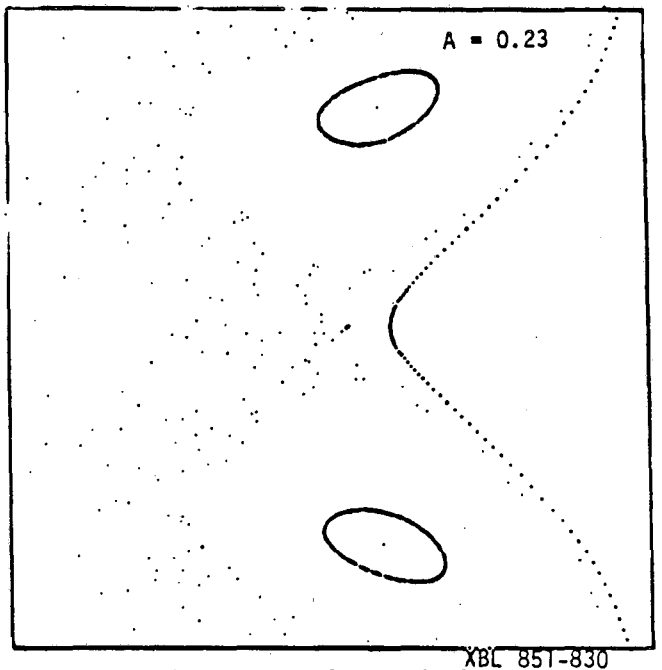

Fig. II.3a Detail related to Fig. II.3 (A=0.23); Scales:
Horizontal: -3.0 to -2.0, for x; Vertical: -0.08 to 0.08, for x'.
Shown are a portion of the apparently limiting trajectory launched with $x_0 = -2.4$, two members of the stable order 7/1 fixed-point system (with surrounding loops), and an unstable sequence of points resulting from a launch substantially at an unstable order 7/1 fixed point.

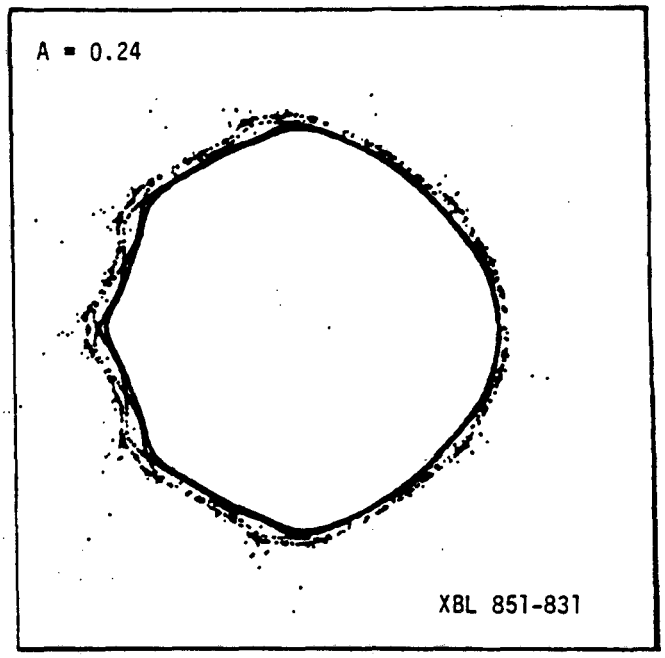

Fig. II.4 Phase Plot for A = 0.24; Scales:
Horizontal -3.25 to 3.25, for x; Vertical: -0.30 to 0.30, for x'.
An apparently stable limiting trajectory is shown that results from a launch with $x_0 = -2.3$, $x_0' = 0$. Features of stable and unstable order 13/2 fixed-point systems also are shown. A run launched substantially at an unstable fixed point of this system ($x_0 = -2.384407_{0663}$, $x_0' = 0$) shows evident stochasticity and a run launched on the x-axis at $x_0 = -2.5$ shows a pronounced blow up in the course of traversing some 714 periods of the structure (see Detail, Fig. II.4a).

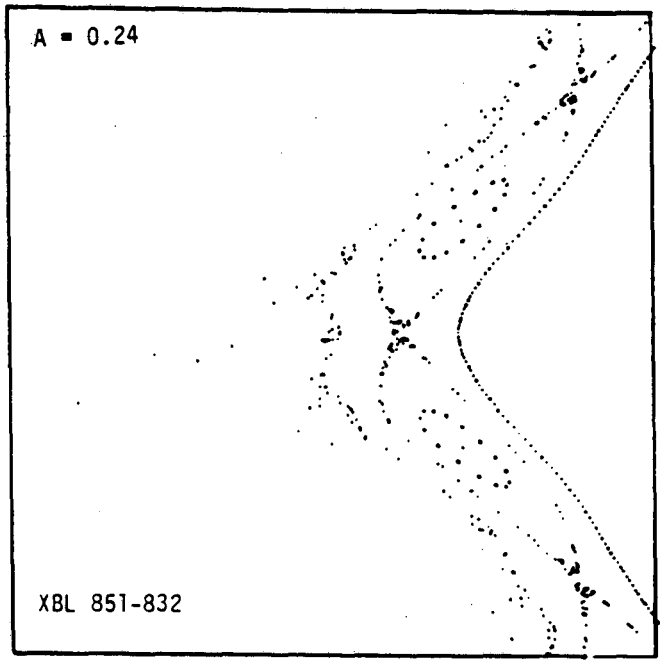

Fig. II.4a Detail related to Fig. II.4 (A = 0.24); Scales:
Horizontal -3.0 to -2.0, for x; Vertical -0.08 to 0.08, for x'.
Shown are a portion of the apparently stable trajectory launched with $x_0 = -2.3$, two members of the stable order 13/2 fixed-point system (with surrounding loops), an evidently stochastic trajectory originating near an unstable order 13/2 fixed point, and the pronounced instability of a run launched on the x-axis at $x_0 = -2.5$ (a small distance beyond the order 13/2 system).

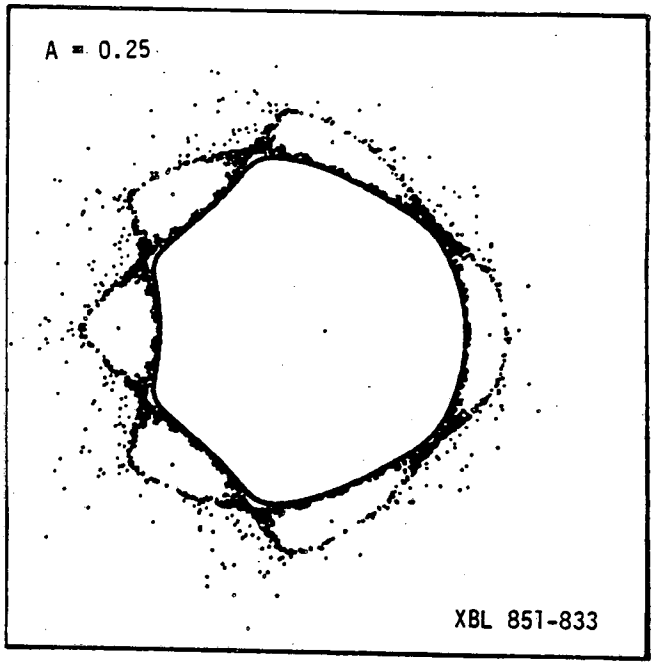

Fig. II.5 Phase plot for A = 0.25; Scales:
Horizontal: -3.25 to 3.25, for x; Vertical: -0.30 to 0.30, for x'.
A limiting apparently stable phase trajectory is shown, as a result of a launch at $x_0 = -1.7$, $x_0' = 0$. Stable order 6/1 fixed points also are shown, together with the results of a clearly stochastic run originating in the immediate neighborhood of an unstable fixed point of the order 6/1 system.

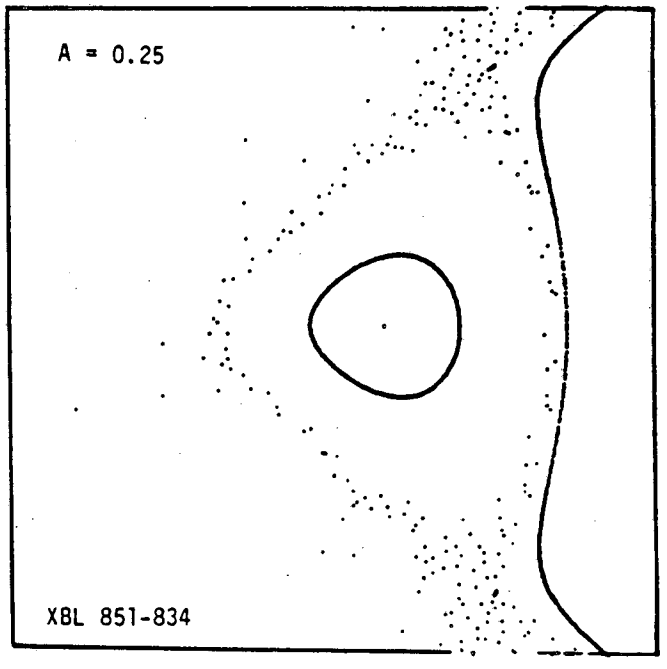

Fig. II.5a Detail related to Fig. II.5 (A = 0.25); Scales:
Horizontal: -3.0 to -1.5, for x; Vertical: -0.08 to 0.08, for x'.
Shown are a portion of the limiting stable trajectory launched with $x_0 = -1.7$, a member of the stable order 6/1 fixed-point system, (with a surrounding small loop), and the stochastic instability resulting from a launch at an unstable fixed point of order 6/1.

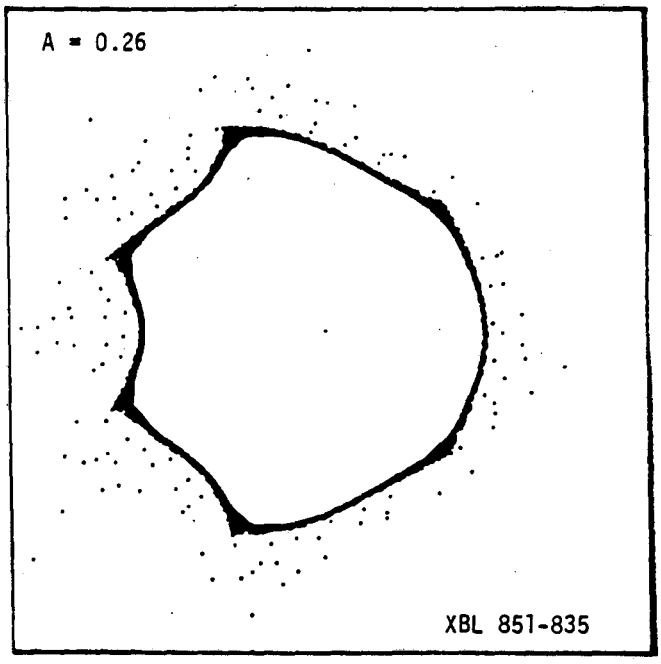

Fig. II.6 Phase plot for A = 0.26; Scales:
Horizontal: -3.25 to 3.25, for x; Vertical: -0.30 to 0.30, for x'.
A limiting apparently stable phase trajectory is shown, as a result of a launch at $x_0 = -1.9$ and $x_0' = 0$. Also shown is a surrounding order 23/4 fixed-point system from which stochastic instability is seen to develop.

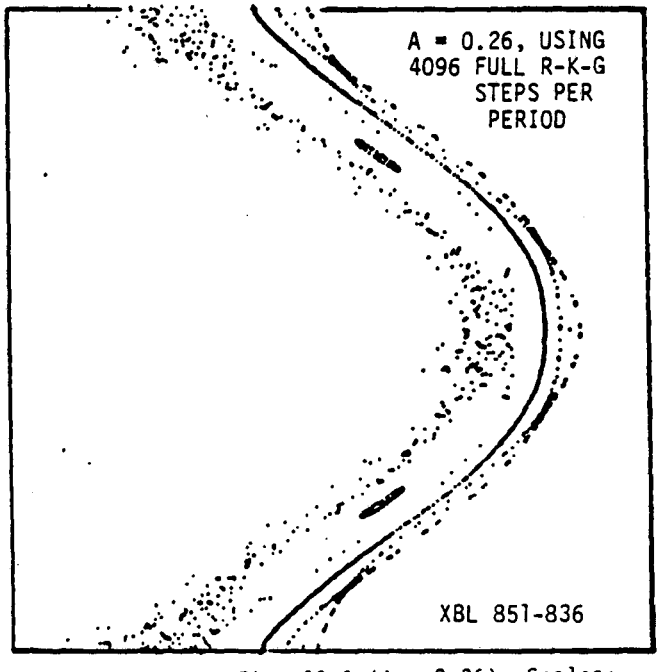

Fig. II.6a Detail related to Fig. II.6 (A = 0.26); Scales:
Horizontal: -2.10 to -1.85, for x; Vertical: -0.05 to 0.05, for x'.
An apparently smooth phase trajectory, originating on the x-axis at $x_0 = -1.89$, is shown and evidently indicates substantially the limit of stability. Portions of an order 40/7 system have been added, at smaller amplitude, to the right of this trajectory segment. At larger amplitude a distinctly stochastic motion, ultimately leading to blow-up, is seen to result from a launch at $x_0 = -1.903935420$ and $x_0' = 0$ from an unstable fixed point of the order 23/4 system.

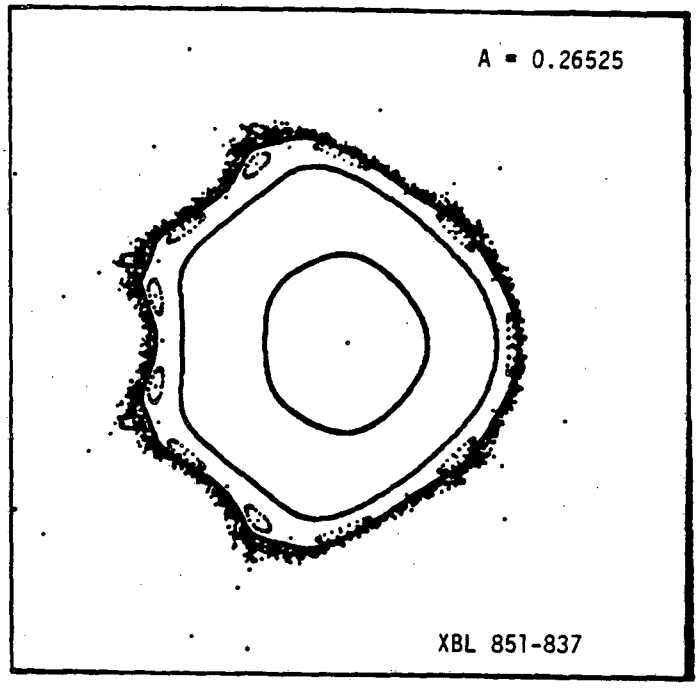

Fig. II.7 Phase plot for A = 0.26525; Scales:
Horizontal: -3.25 to 3.25, for x; Vertical: -0.30 to 0.30, for x'.
For this value of A, the small-amplitude tune is such that σ = 71.963493 deg. When examined on an enlarged scale (see Figs. II.7a-d), several fixed-point systems become evident at amplitudes near to the stability boundary -- e.g., systems of order 11/2, 50/9, 39/7, and 28/5, for which the respective tunes become $\sigma \cong$ 65.4545, 64.80, 64.6154, and 64.2857 degrees. A limiting boundary curve appears to result from a launch with x_0 = -1.86, x_0' = 0, just outside the system of order 50/9, and is shown as the outermost closed curve on this figure (together with two additional closed curves, of considerably smaller amplitudes, that are also shown encircling the origin). The presence of stable fixed points of an order 11/2 system (together with small surrounding loops) and of unstable order 11/2 fixed points also is indicated; some stochasticity may be associated with these unstable order 11/2 fixed points (see Fig. II.7d), but the order 11/2 system is contained within the apparently smooth limiting boundary curve mentioned above. The features of the order 50/9 fixed-point system are not readily depicted on the present rather coarse scale, but one sees an evident instability that results from a run originating near an unstable fixed point of the order 28/5 system (here taken to be at x_0 = -2.05607625, x_0' = 0.0520677).

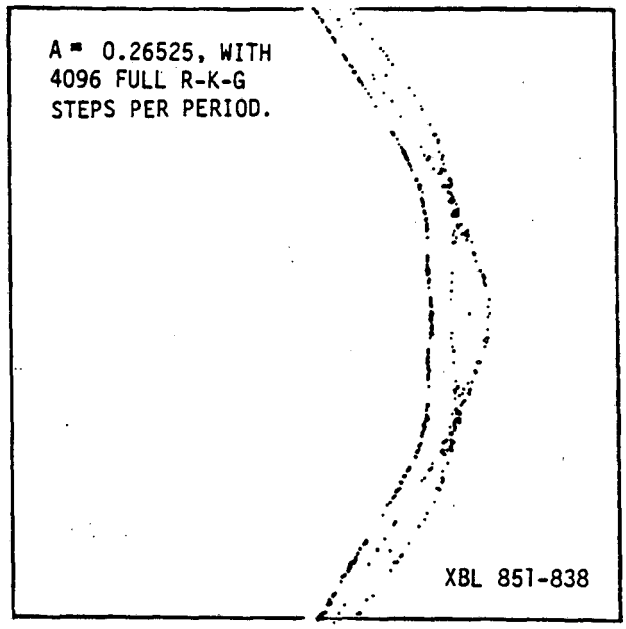

Fig. II.7a Detail related to Fig. II.7 (A = 0.26525); Scales:
Horizontal: -2.00 to -1.80, for x; Vertical: -0.02 to 0.02, for x'.
This figure shows a portion of the presumed smooth "limiting boundary curve" that results from a launch at $x_0 = -1.86$, $x_0' = 0$, and to which reference was made in the caption to Fig. II.7. At smaller amplitudes, to the right of this trajectory segment, one sees portions of order 50/9 fixed-point systems, with some evident stochasticity noticeable in the neighborhood of the unstable fixed points of this system. It of course is a matter of judgement whether the so-called boundary curve, as computed here, is truly sufficiently smooth that phase points are precluded from crossing into regions of larger amplitude.

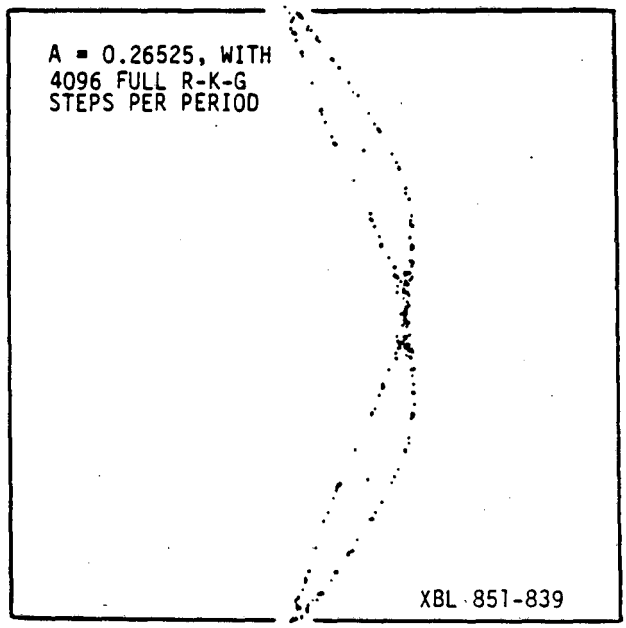

Fig. II.7b Detail related to Fig. II.7 (A = 0.26525); Scales:
Horizontal: -2.00 to -1.80, for x; Vertical: -0.02 to 0.02, for x'.
Portions of order 39/7 fixed-point systems, with evidence of some stochastic behavior in the neighborhood of the unstable fixed point shown for this system.

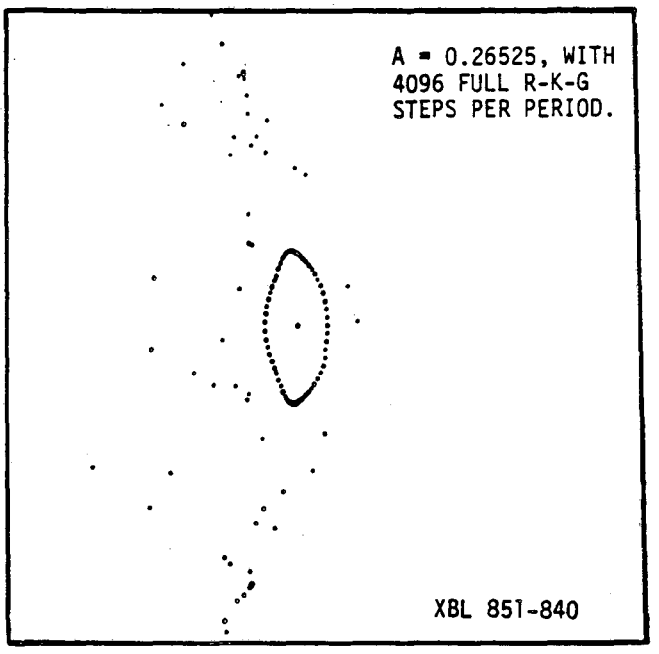

Fig. II.7c Detail related to Fig. II.7 (A = 0.26525); Scales:
Horizontal: -2.00 to -1.80, for x; Vertical: -0.02 to 0.02, for x'.
Highly stochastic instability associated with unstable fixed points of an order 28/5 system, shown together with a stable fixed point (and surrounding loop) of this same order.

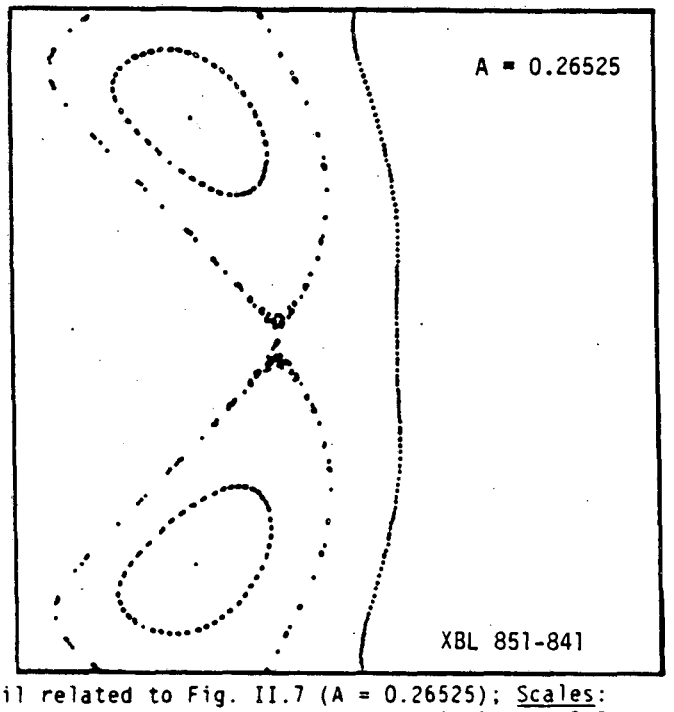

Fig. II.7d Detail related to Fig. II.7 (A = 0.26525); Scales:
Horizontal: -2.00 to -1.50, for x; Vertical: -0.06 to 0.06, for x'.
Detail of fixed points of order 11/2 systems, indicating possible stochasticity near the unstable order 11/2 fixed point. Also shown is a portion of an apparently smooth phase trajectory of somewhat smaller amplitude that results from a launch with $x_0 = -1.7$, $x_0' = 0$.

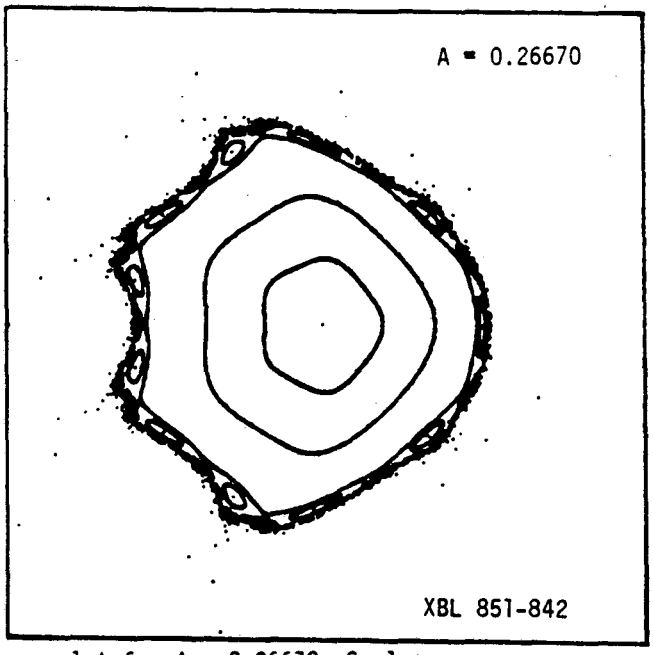

Fig. II.8 Phase plot for A = 0.26670; Scales:
Horizontal: -3.25 to 3.25, for x; Vertical: -0.30 to 0.30, for x'.
Shown is the erratic and clearly unstable phase motion that results from a launch with $x_0 = -1.8377526$, $x_0' = 0$, just beyond an unstable fixed point of order 11/2. Also shown are stable fixed points (and encircling loops) of order 11/2. The limiting closed phase trajectory appears to be that which results from a launch with $x_0 = -1.82$, $x_0' = 0$ -- shown here together with additional curves that encircle the origin with a smaller amplitude.

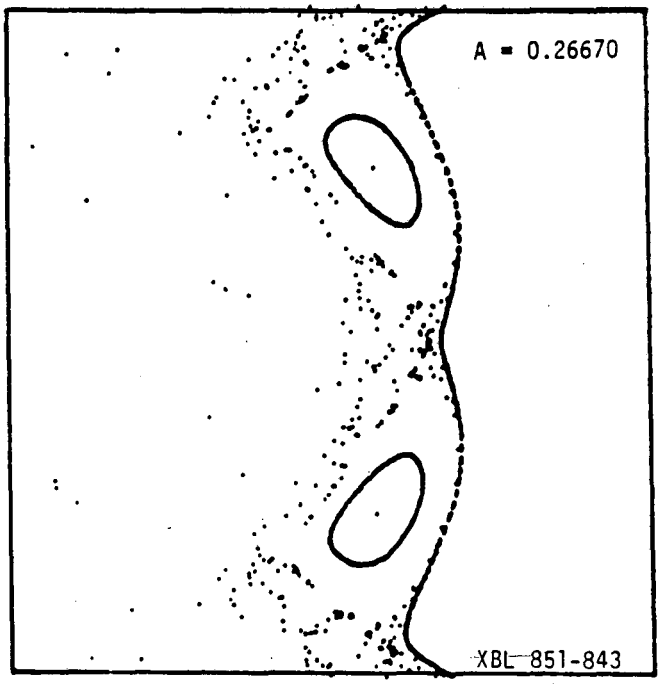

Fig. II.8a Detail related to Fig. II.8 (A = 0.26670); Scales:
Horizontal: -2.50 to -1.50, for x; Vertical: -0.08 to 0.08, for x'.
This detail shows a portion of the apparently smooth curve, resulting from a launch at $x_0 = -1.82$, $x_0' = 0$, that may be regarded as situated at the edge of the region of stability [plotted for 2500 periods]. At only slightly greater amplitude clearly unstable stochastic motion is seen to develop from a launch at an unstable order 11/2 fixed point ($x_0 = -1.83775252$, $x_0' = 0$). Two of the stable order 11/2 fixed points also are shown, together with small surrounding loops.

B.

$$\frac{d^2x}{dZ^2} = -A\,(\,x + 1/12\,x^3 + 1/384\,x^5\,)\cos Z$$

The character of solutions to Eqn.(2) also could be examined in the manner in which solutions to Eqn. (1) were examined in the preceding sub-section. An overall indication of the nature of solutions to Eqn. (2) is shown, for A = 0.2088, in Fig. II.9. With this value of the parameter A, the tune for small-amplitude motion is such that σ_0 = 55.1621 degrees and σ increases with increasing amplitude with the result that a pronounced order 6/1 fixed-point system (σ = 60 deg.) is seen to occur at intermediate amplitudes.

The largest simple, apparently smooth, closed phase trajectory shown on Fig. II.9 resulted from a launch with x_0 = 1.6 and x_0' = 0 ($\sigma \cong$ 68.87 deg.), and shortly beyond this curve systems of order 5/1 fixed points make their appearance. It is of interest to note that there are, in fact, <u>two</u> systems of stable order 5/1 fixed points (and similarly <u>two</u> systems of unstable order 5/1 fixed points). Thus, one system of stable order 5/1 fixed points has one member of this family situated on the positive x-axis ($x \cong 1.782071$) and the remaining four members situated symmetrically above and below the x-axis, while the second family has its members similarly situated save for a reversal of sign for the x-coordinate of each member. With respect to the unstable order 5/1 fixed points, one member of one family is situated on the positive x'-axis ($x' \cong 0.19289322$) with other members of that family symmetrically situated to the right and left of that axis, while the second unstable family is similar save for a reversal of sign of x' for each member. The mapping of phase points in the neighborhood of the unstable order 5/1 fixed points presents, moreover, a distinctly stochastic character, and a run launched on the x-axis with x_0 = 1.89 is found to lead to a gross instability ("blow-up", not shown).

At still larger amplitudes on Fig. II.9 one finally sees the locations of stable and unstable fixed points of order 14/3 ($\sigma \cong$ 77.1429 deg.), with two members of the stable system lying on the x'-axis at $x' \cong \pm 0.22460743$ and two members of the unstable system on the x-axis at $x \cong \pm 1.99832577$. The unstable order 14/3 system is locally very strongly unstable (half trace of tangential-mapping transformation $\cong$ 16.2579), while the stable family (HTR $\cong$ 0.91026484) can be of interest in giving rise to a bifurcation (<u>without</u> period doubling) when the parameter A is slightly reduced (Chapter III).

Figure II.9a shows some detail of the phase plane in the near neighborhood of the stable order 5/1 fixed point situated (as on Fig. II.9) on the x-axis at $x \cong 1.782071$. The outermost trajectories indicate the presence of 11 stable and 11 unstable order 55/11 fixed points, arranged to surround the order 5/1 fixed point situated near the center of this diagram. The stochastic evolution of phase

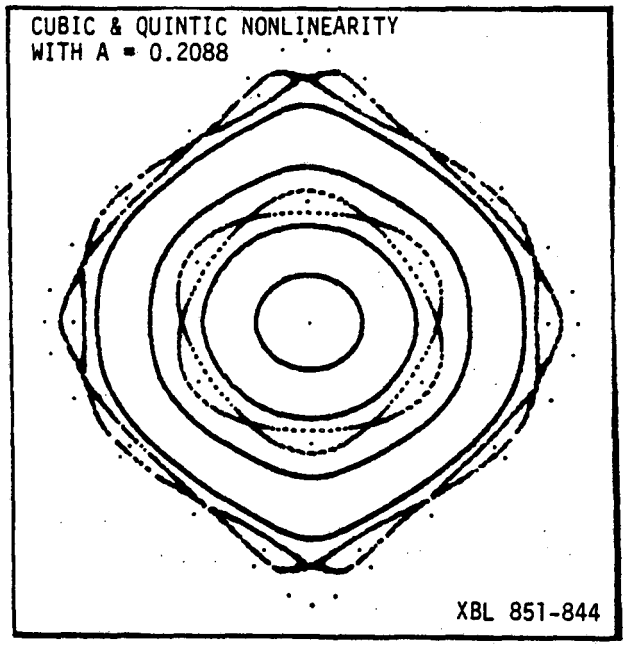

Fig. II.9 Phase plot, at Z = 0 mod. 2π, for solutions to Eqn. (2) with A = 0.2088 (σ_0 = 55.1621 deg.). Scales:
Horizontal: -2.25 to 2.25, for x; Vertical: -0.25 to 0.25, for x'.
Distinctive features include systems of stable and unstable order 6/1 fixed points, two stable and two unstable order 5/1 systems, and the locations of stable and unstable order 14/3 fixed points. The largest simple, apparently smooth, closed phase trajectory originated from a launch with x_0 = 1.6 and x_0' = 0.

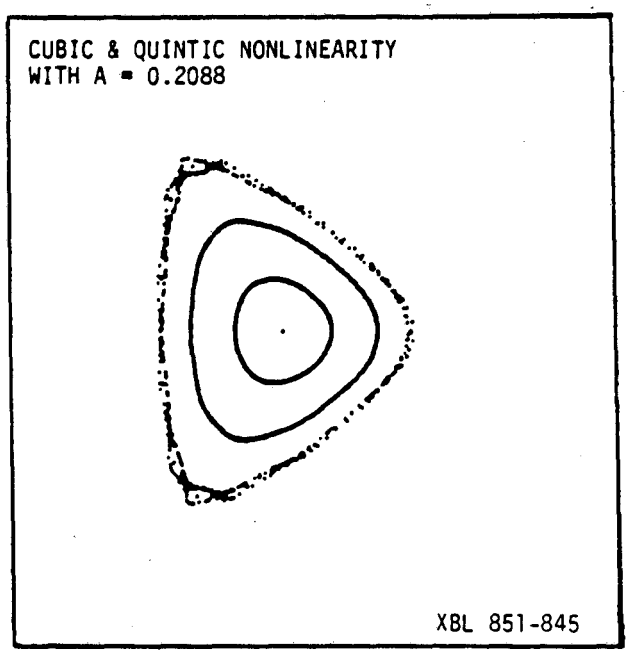

Fig. II.9a Detail related to Fig. II.9, for Eqn.(2) with A = 0.2088, Scales:
Horizontal: 1.60 to 2.00, for x; Vertical: -0.06 to 0.06, for x'.
Phase trajectories surrounding a stable order 5/1 fixed point are shown, together with indications of stable and unstable fixed points of order 55/11 in this vicinity.

points for a run launched near an unstable order 5/1 fixed point (e.g., near x_0 = 1.68129339, x_0' = 0.04744928) would carry such points to regions further removed from the stable order 5/1 fixed point shown here.

REFERENCES OR NOTES

1. A curl-free, divergence-free magnetic field that is longitudinally periodic with period P and is of a quadrupole character with respect to its dependence on ø can be constructed from terms of the form

$$B_r = k\, I_2'(kr) \cos kZ \sin 2\phi$$
$$B\phi = (2/r)\, I_2(kr) \cos kZ \cos 2\phi$$
$$B_Z = -k\, I_2(kr) \sin kZ \sin 2\phi \quad ,$$

   with k any integer multiple of $2\pi/P$. The nonlinearities necessarily introduced thereby into median-plane motion (ø = 0) accordingly are such as arise from terms of the form $I_2(kr)/r$.

2. Convergence to a numerical evaluation of phase-plane coordinates for fixed points of interest, and the evaluation of the local tune or stability characteristics for small-amplitude oscillations about the periodic orbit corresponding to any such fixed point, can make use conveniently of the "tangential-mapping transformation" that tracks an infinitesimal displacement (δx, $\delta x'$) through the appropriate interval in Z. For other phase trajectories, estimates of tune are obtainable by the technique of counting axis crossings in the x, x' phase plane.

III. BIFURCATION -- ILLUSTRATIONS

For Area-Preserving Transformations and Solutions to Differential Equations

A distinct change can occur in the nature of the fixed-point systems characterizing area-preserving transformations, or solutions to canonical differential equations, as a parameter of the transformation is changed. One finds such changes to occur when a fixed-point system that previously was locally stable becomes unstable as a result of a parameter change and new (stable) fixed points split off to make their appearance. In cases such that the previously stable system becomes unstable with reflection, the new system is found to have a period twice that of its predecessor. A sequence of such period-doubling bifurcations, occurring for smaller and smaller changes of the governing parameter, results in a bifurcation lattice or "tree" that may be claimed to terminate in "chaos".

Illustrations of bifurcation are conveniently obtained by examination of simple area-preserving algebraic mappings,[1] and also can be found in phase-plane mappings that represent solutions to canonical differential equations characteristic of median-plane motion in alternating-gradient particle accelerators or storage rings.

A. An Area-Preserving Quadratic Mapping

The area-preserving quadratic mapping (M)

$$\left.\begin{aligned} x_{n+1} &= y_n + F(x_n) \\ y_{n+1} &= -x_n + F(x_{n+1}) \end{aligned}\right\} , \tag{1}$$

with $F(x) = Tx + (1-T)x^2$ [a generalized deVogelaere form, with parameter T], serves conveniently to illustrate the development of a sequence of period-doubling bifurcations as the parameter T is varied. The transformation (1) results in phase diagrams that exhibit a convenient symmetry about the x-axis. For $|T| < 1$ the origin constitutes a stable first-order fixed point and the point (1, 0) is an unstable first-order fixed point.

For T somewhat negative, phase points representing small-amplitude motion encircle the origin somewhat more rapidly than once per four iterations ($\cos^{-1} T > 90$ deg.), but at larger amplitudes one can find solutions that are locked into order -4/1 fixed-point systems. Such order - 4/1 fixed-point systems are illustrated on Fig. 1 for T = -0.1030. The half-trace (HTR) for the tangential-mapping transformations, for M^4 linearized about a stable fixed point of the system,[2] then may be computed to be circa -0.9883_{57} -- so that while this fixed-point system is stable, it is close to being unstable with reflection. It accordingly becomes of interest to examine the structure of the phase-space diagram, in the vicinity of such a stable fixed point as that seen in Fig. III.1

to lie on the positive x-axis, as the parameter T is varied (to become somewhat more negative).

For T = -0.1030 (as in Fig. III.1) the character of the phase trajectories in the neighborhood of the stable order - 4/1 fixed point on the positive x-axis is shown to an enlarged scale on Fig. III.2. One notes close to this stable fixed point the occurrence of apparently smooth surrounding phase trajectories that indicate the general nature of flow under action of M^4 in this region of phase space.

For T assigned the slightly more negative value T = -0.1034, the order - 4/1 fixed point on the positive real axis not only shifts its location slightly but, more significantly, becomes locally unstable, with reflection (HTR < -1). Because of this local instability, phase points tend to move away from (or toward) the fixed point, along eigenvector directions, while jumping from one side of the fixed point to the other in the manner characteristic of motion in the neighborhood of a hyperbolic fixed point with reflection (negative eigenvalues). The general circulatory character that was noted earlier for flow in this region evidently remains, however, to take effect at an appreciable distance from the fixed point and results in the diagrams shown (for T = -0.1034) on Fig. III.3 and (to a further enlarged scale) on Fig. III.4.

New (stable) fixed points are seen to occur within the loops of the "lazy-8" features that Figs. III.3 and III.4 show developing from the unstable fixed point. Because the unstable fixed point is unstable <u>with reflection</u> (under action of M^4), the phase-space coordinates will jump from one of these new stable fixed points to the other under action of M^4. The new fixed-point system (of which two members are seen on each of Figs. III.3 and III.4) thus constitutes a system of order - 8/1 (period = 8) and illustrates the occurrence of a period-doubling bifurcation.

It is of some interest to note the qualitative change in character of a diagram such as Fig. III.4 when further reductions are made in the parameter T. Such a change is illustrated by Figs. III.5 - III.14, with T = -0.11125 for the final Figure of this sequence. One notices, in progressing through this sequence, the development of an increasingly pronounced stochasticity about the unstable order - 4/1 fixed points and an enlargement of the area of the lazy-8 loops that surround the stable order - 8/2 fixed points.

When the existence of the order - 8/2 fixed-point system first became apparent (<u>e.g.</u>, for T = -0.1034), the half-trace of the tangential-mapping transformation for the order - 4/1 system was just slightly more negative than -1 (for M^4) and the half trace for the new order - 8/2 system was just slightly less than +1 (for M^8). With selection of increasingly negative values of the parameter T, the half-trace for the order - 4/1 system becomes driven to increasingly negative values and the half-trace of the order - 8/1 system is driven from values near +1 downward toward the critical value HTR = -1.

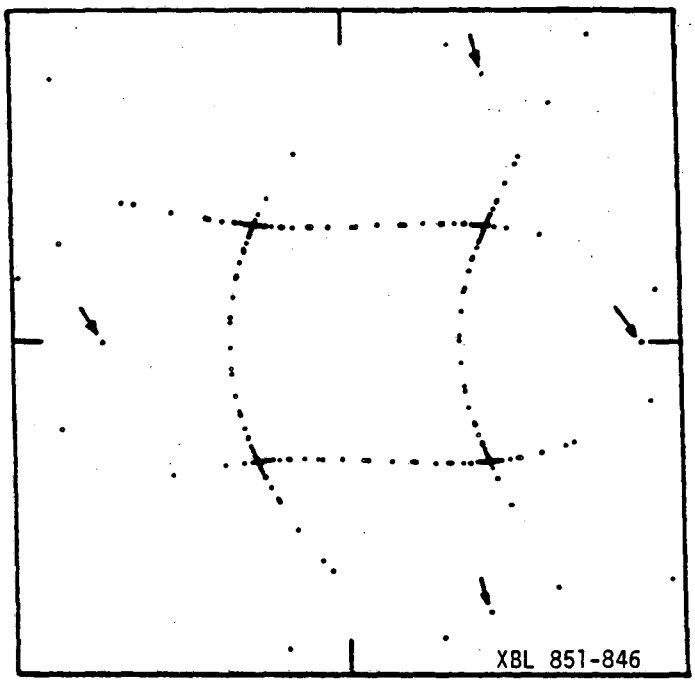

Fig. III.1 T = -0.1030. De-Vogelaere Variables. Scales: -0.60 to +0.60. Locations of 4-th Order unstable and stable fixed points. The 4 stable fixed points are indicated by arrows. We shall follow the behavior in the neighborhood of the fixed point on the positive x-axis (x = 0.532268206310) as T becomes more negative.

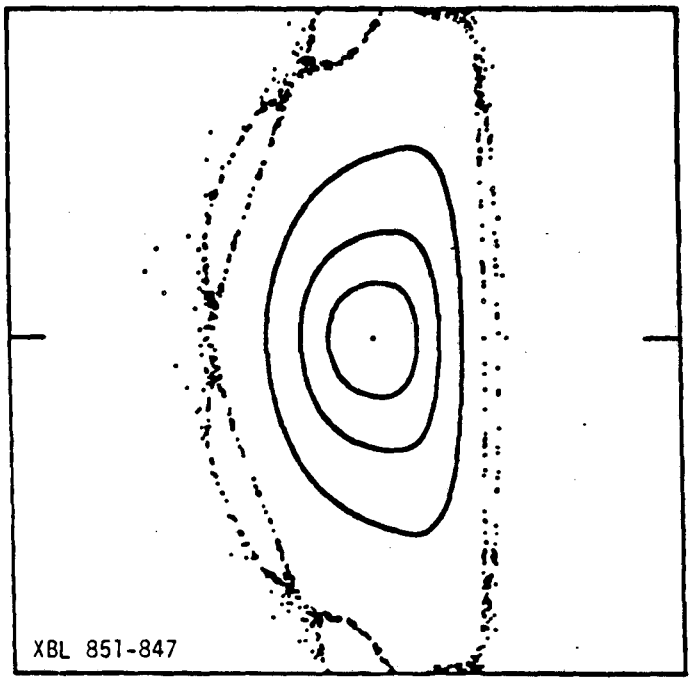

Fig. III.2. T = -0.1030. De-Vogelaere Variables. Enlarged plot of neighborhood about stable fixed point on the positive x-axis (x-scale: 0.45 to 0.60).

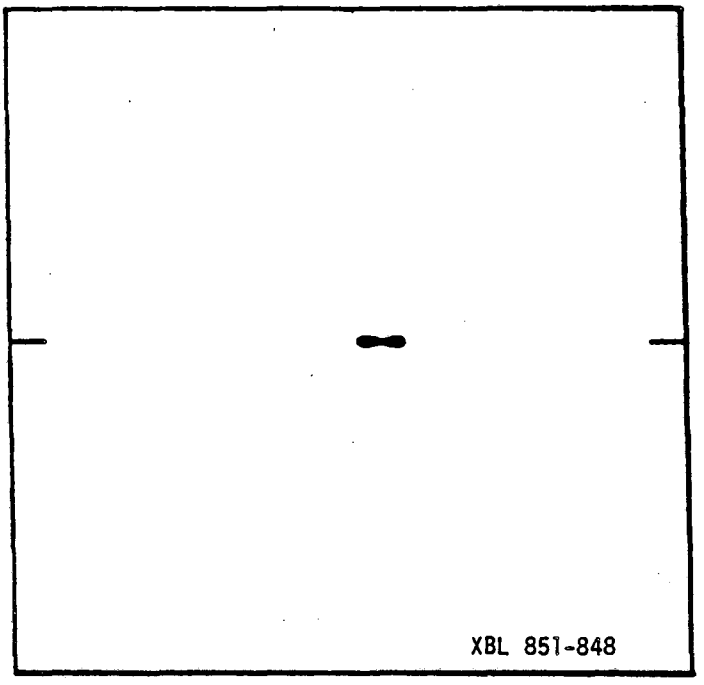

Fig. III.3 T = -0.1034. De-Vogelaere Variables. Scales: 0.45 to 0.60; ±0.003.
Development of bifurcation 1/4: Unstable
2/8: Stable

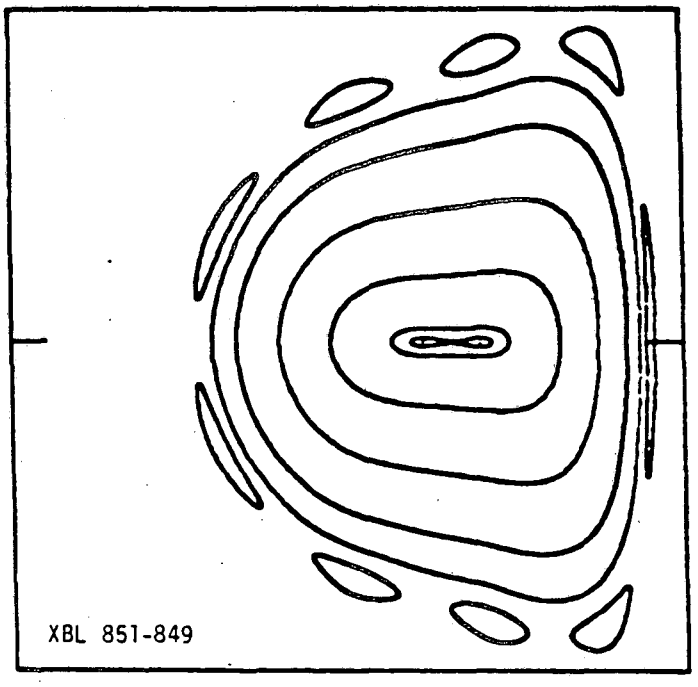

Fig. III.4 T = -0.1034. De-Vogelaere Variables. Scales: 0.48 to 0.56; ±0.0025.
Enlarged view of bifurcation.

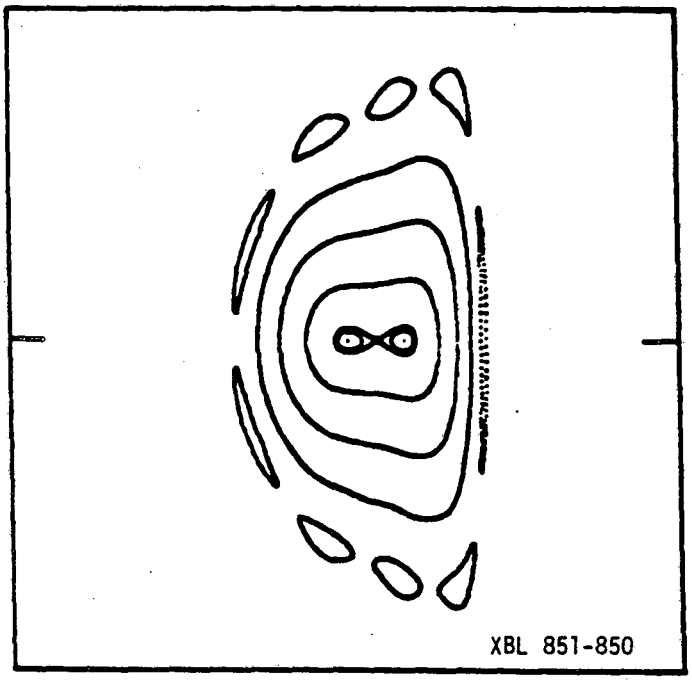

Fig. III.5 T = -0.1035. De-Vogelaere Variables. Scales: 0.45 to 0.60; ±0.003.

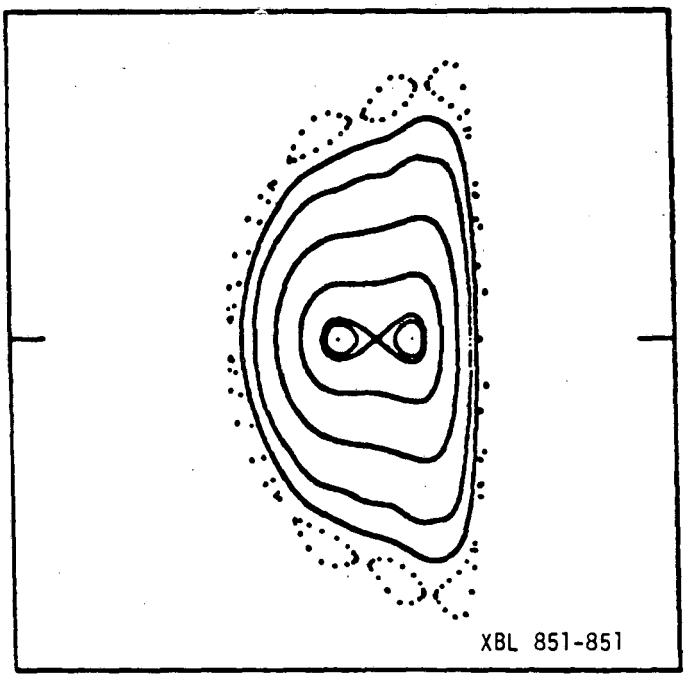

Fig. III.6 T = -0.0136. De-Vogelaere Variables. Scales: 0.45 to 0.60; ±0.003.

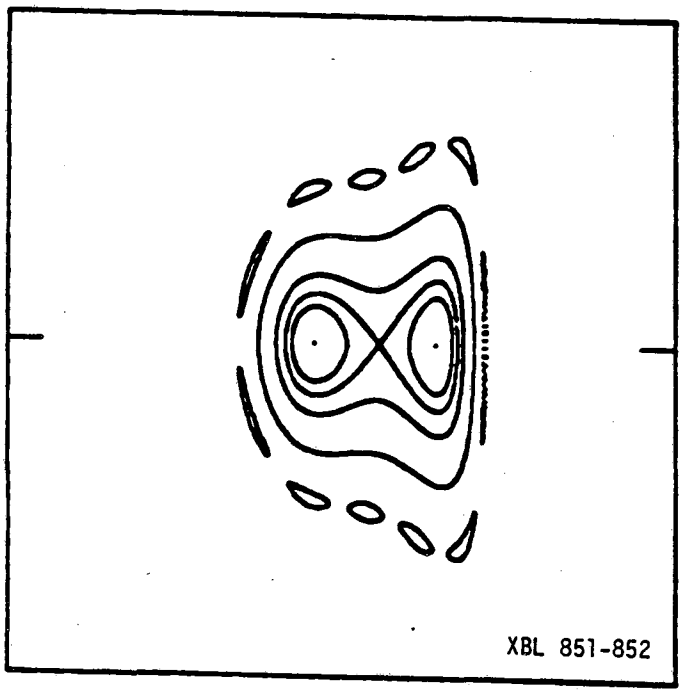

Fig. III.7 T = -0.1040. De-Vogelaere Variables. Scales: 0.45 to 0.60; ±0.003. Note extensions of eigenvector directions from the unstable fixed point appear to form smooth closed curves.

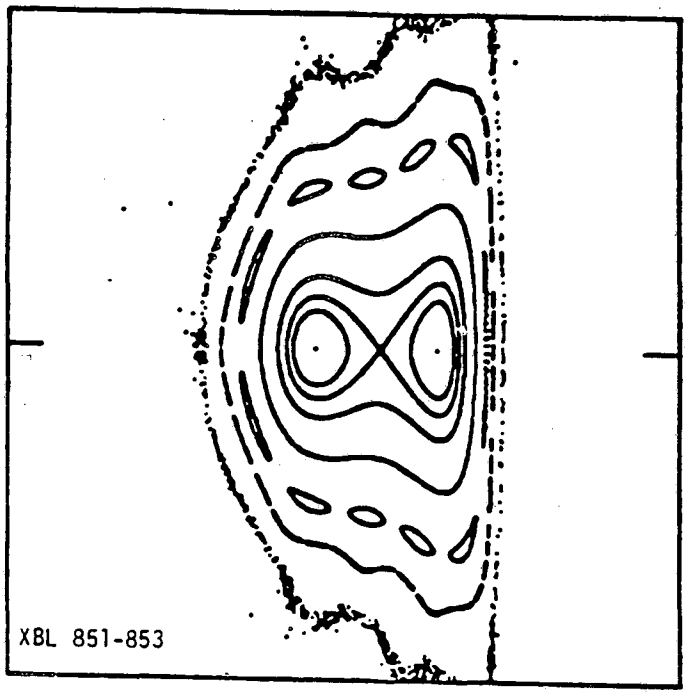

Fig. III.8. T = -0.1040. De-Vogelaere Variables. Scales: 0.45 to 0.60; ±0.003. Plot with inclusion of stochastic boundary.

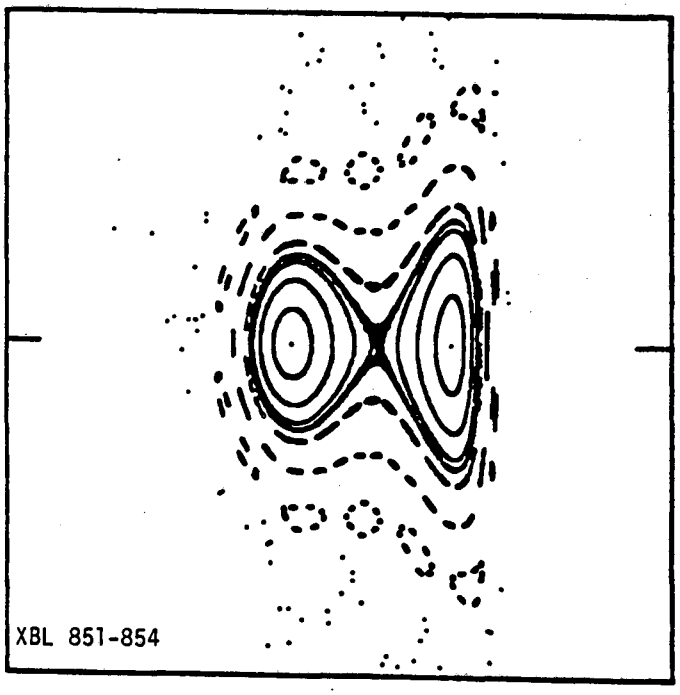

Fig. III.9. T = -0.1045. De-Vogelaere Variables. Scales: 0.45 to 0.60; ±0.003. Note development of evident stochasticity about the unstable fixed point at x = 0.534416773867.

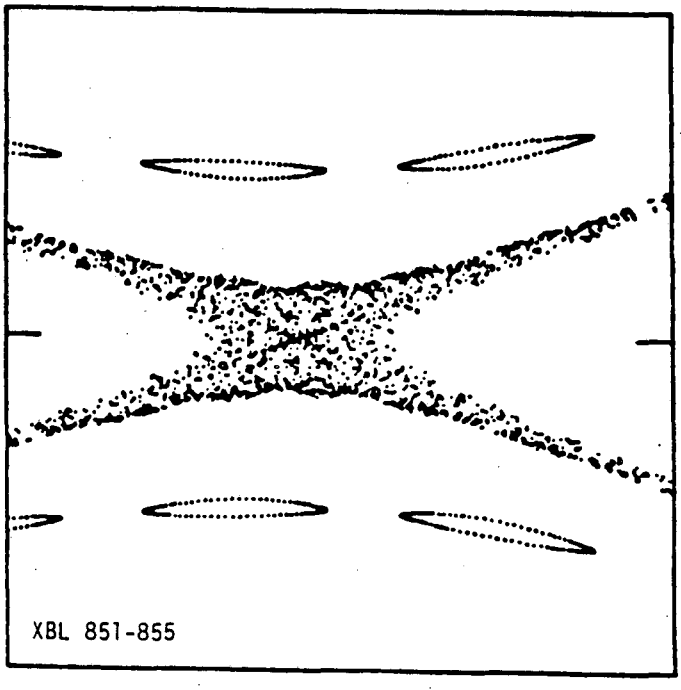

Fig. III.10. T = -0.1045. De-Vogelaere Variables. Scales: 0.53 to 0.54; ±0.001. Detail -- to emphasize stochastic region about the unstable fixed point at x = .534416773867.

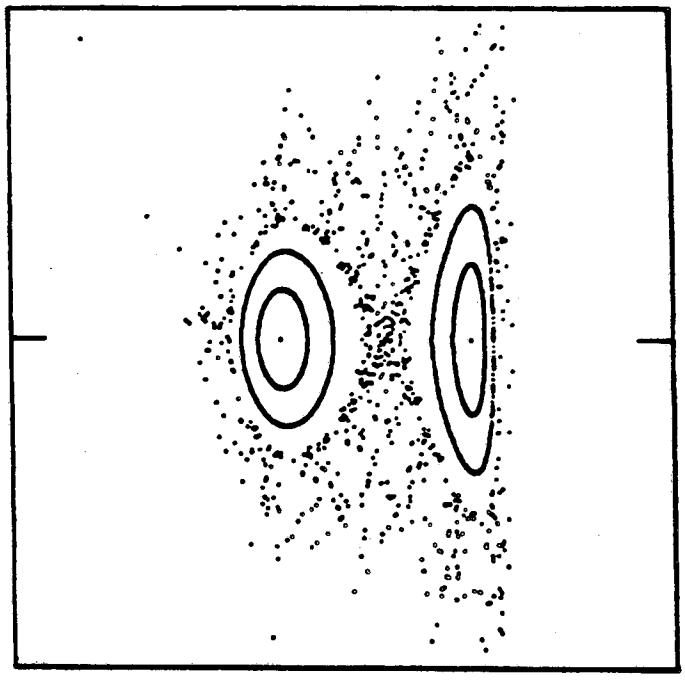

Fig. III.11. T = -0.1050. De-Vogelaere Variables. Scales: 0.45 to 0.60; ±0.003. Note the violent instability at the fixed point (x = 0.535127642205). XBL 851-856

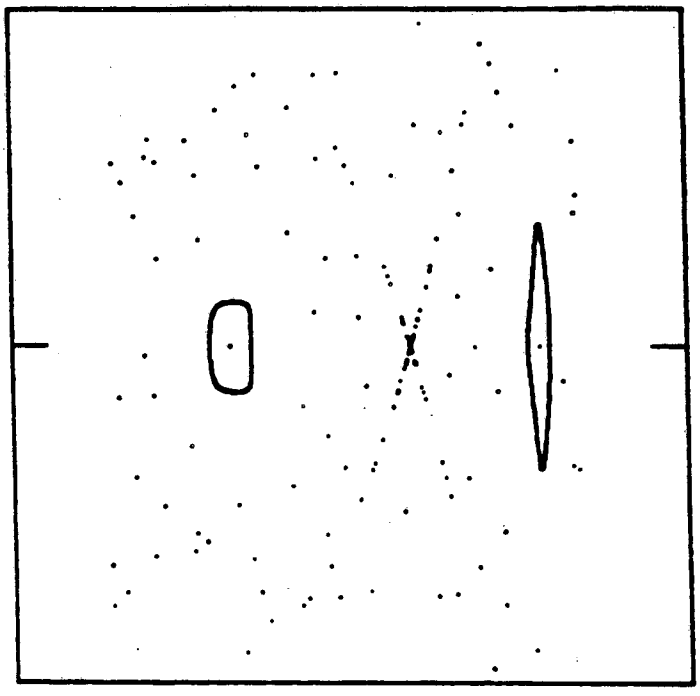

Fig. III.12. T = -0.1075. De-Vogelaere Variables. Scales: 0.45 to 0.60; ±0.003. Some stochastic points, associated with the unstable fixed point, are shown (x = 0.538642977693 for this fixed point). Also shown are two of the stable 8-th order fixed points, together with a surrounding phase trajectory. XBL 851-857

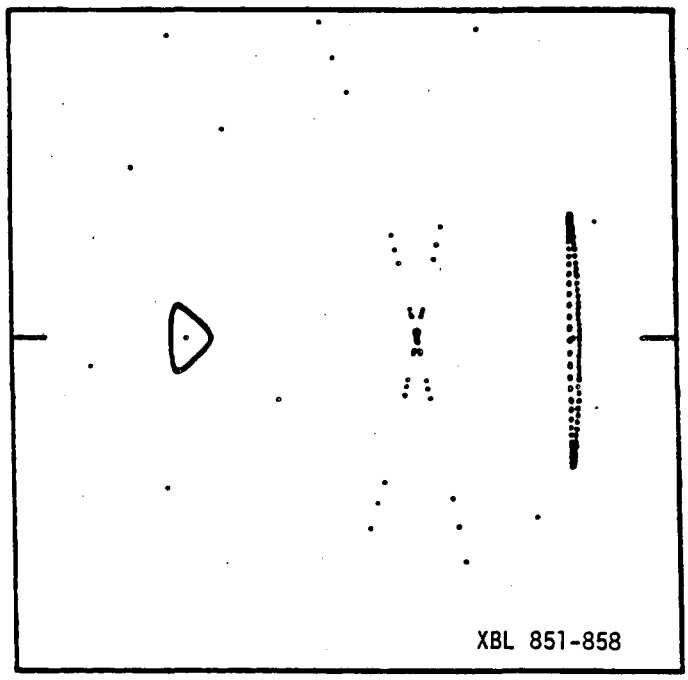

Fig. III.13. T = -0.1100. De-Vogelaere Variables. Scales: 0.45 to 0.60; ±0.003.

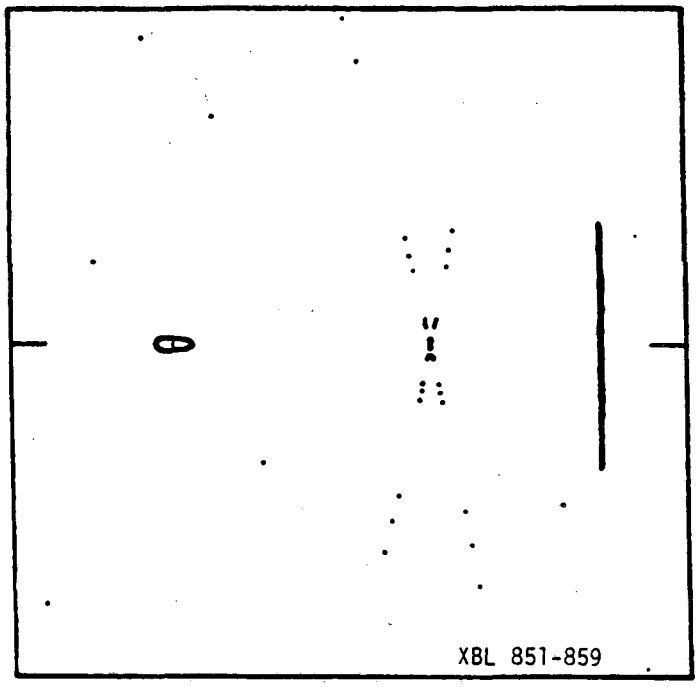

Fig. III.14. T = -0.11125. De-Vogelaere Variables. Scales: 0.45 to 0.60; ±0.003. Neighborhood of 4th order (unstable) and 8-th order (stable) fixed points just prior to additional bifurcation.

For T = -0.11126, the order - 8/2 fixed points have themselves become unstable (HTR < -1 for M^8) and generate loops within which new fixed points of an order - 16/4 system can be found. Such loops are illustrated in Figs. III.15 and III.16 for fixed points situated on the positive x-axis near x = 0.581 and x = 0.486.

Following this second bifurcation, a further reduction of T leads to a third period-doubling bifurcation, generating a fixed-point system of order - 32/8, that is illustrated for T = -0.11223 by Figs. III.17 and III.18.

As new stable fixed-point systems become created and then are driven toward instability (with reflection) by continued change of the parameter T, a regular convergent sequence of successive period doublings appears to become established -- as is suggested schematically by the sketch of Fig. III.19. Some sequential regularity in the locations or separations of the fixed points also may develop, as is indicated for the present example by the bifurcation tree shown in Fig. III.20 to depict the locations of such fixed points as are situated on the positive x-axis. Under circumstances such that a sequence of this nature has been carried to completion, one may expect the phase-plane motion in such a region to appear particularly "chaotic".

B. A Differential Equation with Quadratic Nonlinearity

The differential equation

$$\frac{d^2x}{dZ^2} = -A\,(x + 1/8\,x^2)\,\cos Z, \qquad (2)$$

that has been used to show the effect of a quadratic nonlinearity, can be used to provide solutions that illustrate the occurrence of bifurcations. Such examples include, for the parameter A in the range 0.265 < A < 0.275, fixed-point systems that develop from fixed points of order 6/1 (tune: σ = 1 X 360/6 = 60 deg.) and of order 11/2 (tune: 2 X 360/11 = 65.45...deg.).

It must be stated, with respect to each of the systems mentioned, that the bifurcation process occurs somewhat outside of the normal region of stability in the x, x' phase plane. Thus, with A = 0.2651, for which the small-amplitude tune is $\sigma_0 \cong 71.9167$, the range of stable motion may be judged to be given by -1.93 < x < 1.67 (measured for x' = 0, at Z = 0 mod. 2π) and the tune has dropped to $\sigma \cong$ 64 deg. at such amplitudes. With this value of A, two members of the stable order - 6/1 fixed-point system that is close to becoming unstable and generating a period-doubling bifurcation, lie on the x-axis at x = -2.6916782 and at x = 2.0097530. Similarly, with A = 0.2735 ($\sigma_0 \cong 74.5570$) the range of stability may be estimated as lying within the limits -1.72 < x < 1.64 and the tune has dropped to $\sigma \cong$ 68.1 deg. at such amplitudes. With this value of A, one member of the stable order - 11/2 fixed-point system that is close to giving rise to a period-doubling bifurcation lies on the positive x-axis at x = 1.80151231.

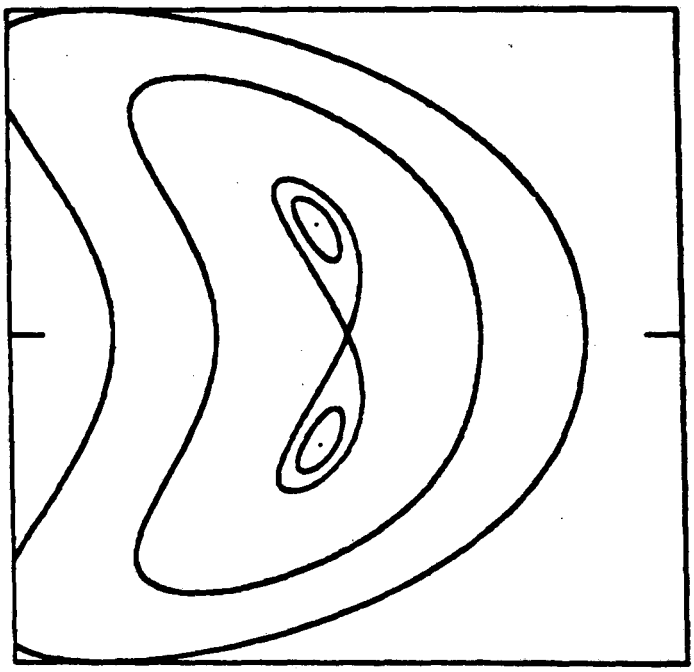

Fig. III.15. T = -0.11126. De-Vogelaere Variables. Scales: 0.581340 to 0.581355; ±0.0002. After the second bifurcation (leading to Order-16 fixed points), one of the (now unstable) Order-8 fixed points develops vertical loops, that contain stable Order-16 fixed points. The fixed points shown are 2/8: 0.581347619364, 0. 4/16: 0.581346959845, ±0.000068014914. XBL 851-860

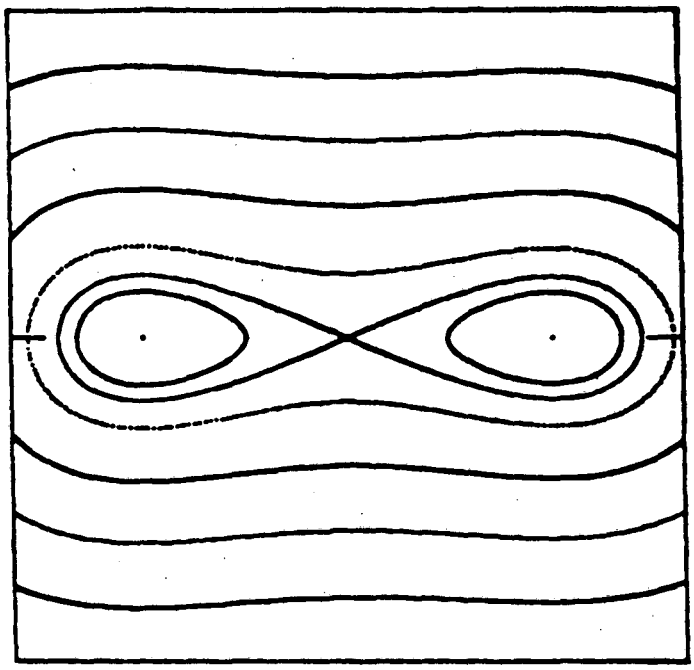

Fig. III.16 T = -0.11126. De-Vogelaere Variables. Scales: 0.4852 to 0.4860; ±0.000001. After the second bifurcation (leading to Order-16 fixed points), one of the (now unstable) Order-8 fixed points develops horizontal loops, that contain stable Order-16 fixed points. The fixed points shown are 2/8: 0.485601872680, 0. 4/16: 0.485356977954, 0, 0.485849305665, 0. XBL 851-861

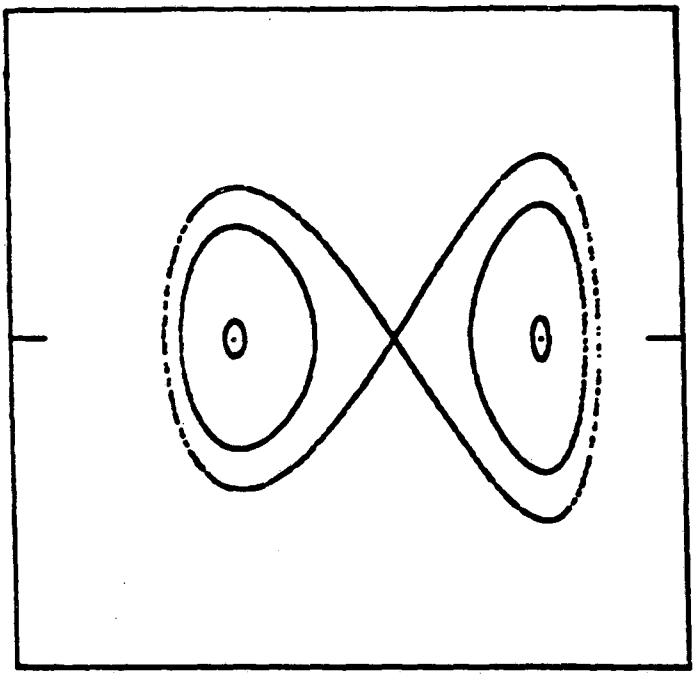

Fig. III.17. T = -0.11223. De-Vogelaere Variables. Scales: 0.4965 to 0.4990; ±0.000002. After the third bifurcation (leading to Order-32 fixed points), one of the (now unstable) Order-16 fixed points develops horizontal loops, that contain stable Order-32 fixed points. The fixed points shown are 4/16: 0.497936225267, 0. 8/32: 0.497335279454, 0, 0.498484243334, 0. XBL 851-862

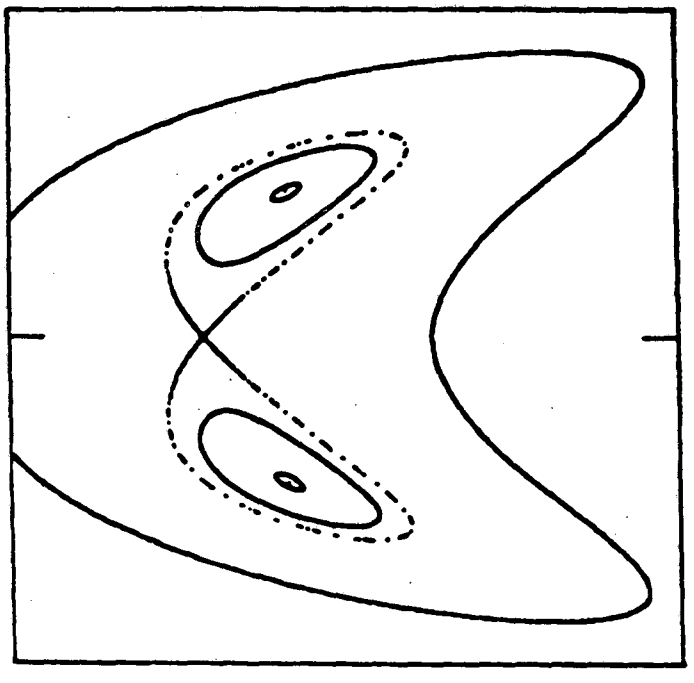

Fig. III.18. T = -0.11223. De-Vogelaere Variables. Scales: 0.4737 to 0.4738; ±0.0001. After the third bifurcation (leading to Order-32 fixed points), one of the (now unstable) Order-16 fixed points develops vertical loops, that contain stable Order-32 fixed points. The fixed points shown are 4/16: 0.473728930908, 0. 8/32: 0.473741772757, ±0.000044371638. XBL 851-863

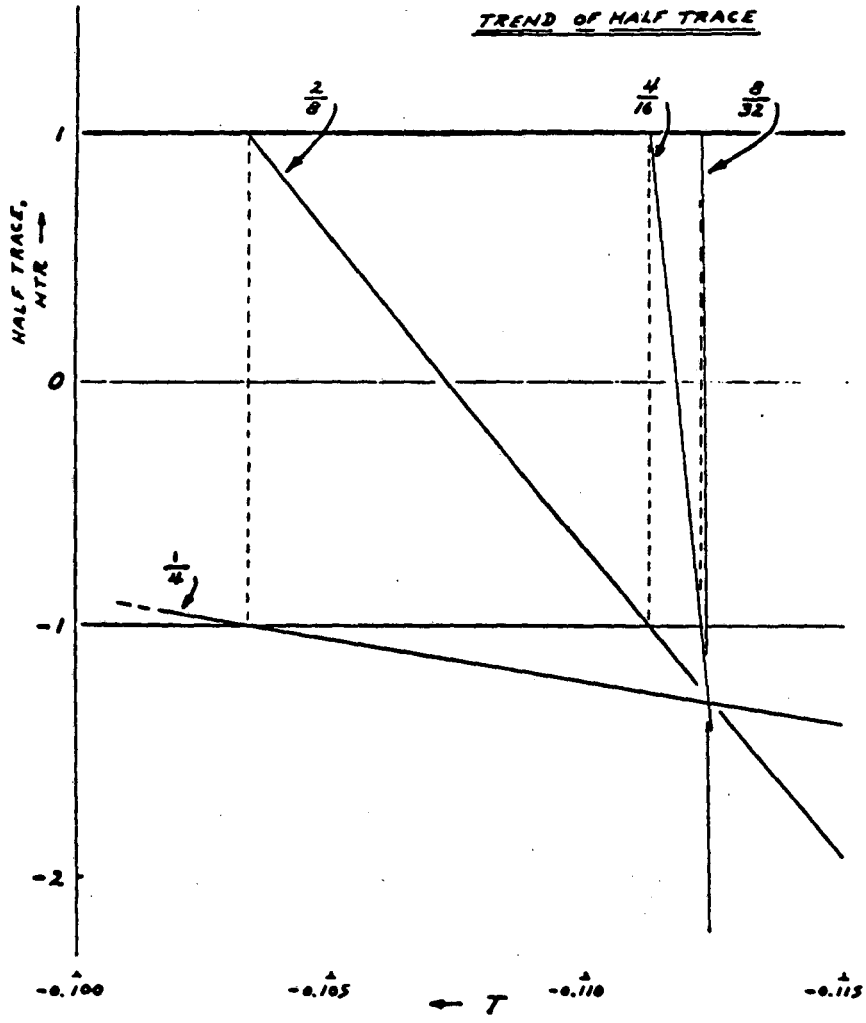

Fig. III.19.
XBL 851-867

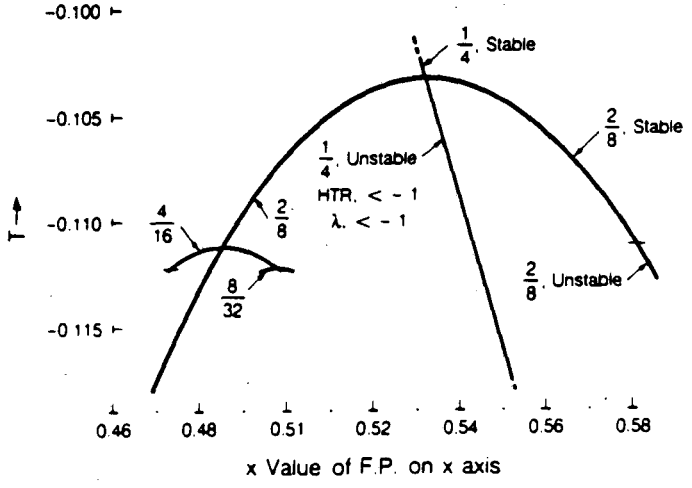

Fig. III.20.
XBL 851-9720

Characteristics of fixed-point systems of order-6/1 are listed in Table I for $0.2650 \leq A \leq 0.2670$, together with the values of small-amplitude tune (σ_0) associated with these values of A. The values given for HTR refer to the half trace of the tangential-mapping transformation (for 6 periods, $\Delta Z = 6(2\pi)$). For the unstable systems with HTR > +1, phase-plane coordinates are given as x_0, $\pm x_0'$ for such order-6/1 fixed-points lying close to the negative x-axis. For the systems with HTR < +1, x coordinates are given for the members of such systems that lie on the negative x-axis and for the members that lie on the positive x-axis. It is this latter type of fixed-point system for which, when HTR becomes less than -1, the order-6/1 system becomes unstable with reflection and an additional (originally stable) system of order 12/2 becomes created. x-values for fixed points of such a fixed-point system, and that lie on the negative x-axis, are tabulated in Table II (together with the half trace of the 12-period tangential-mapping transformation). Such an order 12/2 system will in turn become unstable, with reflection, for A sufficiently great -- leading to a fixed point system of order 24/4. Fixed points situated on the negative x-axis are given in Table III for a few values of the parameter A, and it is seen that one may expect a further period-doubling bifurcation to develop from this order - 24/4 system for values of A slightly greater than 0.266847.

TABLE I Order-6/1 Systems

A	Small-Amp'l. Tune, σ_0 (Deg.)	HTR > +1			HTR < +1		
		x_0	$\pm x_0'$	HTR	x_{left}	x_{right}	HTR
0.2650	71.8856	-2.343555	0.072379	2.409455	-2.688509	2.008182	-0.980123
0.2651	71.9167	-2.346288	0.072410	2.421250	-2.691678	2.009753	-0.998529
0.2652	71.9479	-2.349017	0.072441	2.433116	-2.694840	2.011317	-1.017065
0.2653	71.9791	-2.351741	0.072472	2.445054	-2.697996	2.012874	-1.035730
0.2654	72.0103	-2.354459	0.072502	2.457065	-2.701145	2.014424	-1.054527
0.2655	72.0415	-2.357173	0.072533	2.469148	-2.704288	2.015968	-1.073454
0.2657	72.1039	-2.362587	0.072593	2.493531	-2.710553	2.019035	-1.111705
0.2660	72.1975	-2.370672	0.072682	2.530658	-2.719902	2.023585	-1.170082
0.2665	72.3538	-2.384051	0.072827	2.594021	-2.735355	2.031037	-1.270082
0.2666	72.3850	-2.386713	0.072856	2.606920	-2.738426	2.032508	-1.290493
0.2667	72.4163	-2.389371	0.072884	2.619894	-2.741491	2.033972	-1.311043
0.2670	72.5101	-2.397315	0.072969	2.659276	-2.750648	2.038326	-1.373531

TABLE II Order - 12/2 System, incl. FP's on negative x-axis

A	x_1	x_2	HTR
0.2652	-2.738676	-2.646999	0.864839
0.2653	-2.759982	-2.627668	0.720072
0.2654	-2.776328	-2.613297	0.577487
0.2655	-2.790168	-2.601434	0.437093
0.2657	-2.813553	-2.582010	0.162918
0.2660	-2.842510	-2.559010	-0.231660
0.2665	-2.882070	-2.529416	-0.844114
0.2666	-2.889138	-2.524347	-0.959735
0.26662	-2.890526	-2.523360	-0.982582
0.26663	-2.891216	-2.522870	-0.993971
0.26664	-2.891904	-2.522381	-1.005336
0.26665	-2.892591	-2.521895	-1.016678
0.2667	-2.895992	-2.519495	-1.073042
0.2670	-2.915447	-2.506055	-1.398966

TABLE III Order 24/4 System, incl. FP's on negative x-axis

A	x_1	x_2	HTR
0.26664	-2.529700	-2.515630	0.95723
0.26665	-2.535224	-2.510339	0.86600
0.26670	-2.549481	-2.497244	0.40488
0.26675	-2.558737	-2.489151	-0.06446
0.26680	-2.566240	-2.482813	-0.54199
0.26684	-2.571515	-2.478471	-0.92988
0.266843	-2.571891	-2.478165	-0.95918
0.266844	-2.572015	-2.478064	-0.96896
0.266846	-2.572264	-2.477862	-0.98851
0.266847	-2.572388	-2.477761	-0.99830
0.266848	-2.572512	-2.477661	-1.0081
0.26685	-2.572759	-2.477461	-1.028

Figure III.21, sketched for A = 0.2667, indicates the locations of such associated fixed points as lie in the neighborhood of the order - 6/1 fixed point situated on the negative x-axis at x = -2.741491. This plot is to the scales:

Horizontal: -3.0 to -2.4, for x; Vertical: -0.002 to 0.002, for x'.

The fixed points shown on the negative x-axis are explicitly:

For order - 6/1 system: $\dot{x} = -2.741491$

For order - 12/2 system: $\dot{x} = -2.895992$ & $x = -2.519495$

For order - 24/4 system: $\dot{x} = -2.549481$ & $x = -2.497244$

The development of the order - 12/2 system is illustrated by Figs. III.22 - III.24, each plotted to the scales:

Horizontal: -3.0 to -2.5, for x; Vertical: -0.005 to 0.005, for x'.

Fig. III.22, for A = 0.2651, shows the order - 6/1 fixed point (stable for this value of A) at $x_o = -2.691678...$, $x'_o = 0$, together with two surrounding phase trajectories.

Fig. III.23, for A = 0.2652, shows the order - 6/1 fixed point (now unstable, for this value of A) and two of the order - 12/2 fixed points that result from the period-doubling bifurcation. Also evident is the presence of nine small order - 54/9 islands surrounding the fixed points in this region of the phase plane.

Fig. III.24, for A = 0.2653, presents a diagram similar to that shown (for A = 0.2652) in Fig. III.23, wherein the unstable order - 6/1 fixed point and two order - 12/2 stable fixed points are again seen and for which some stochasticity appears evident in the neighborhood of the unstable fixed points of the order - 54/9 system.

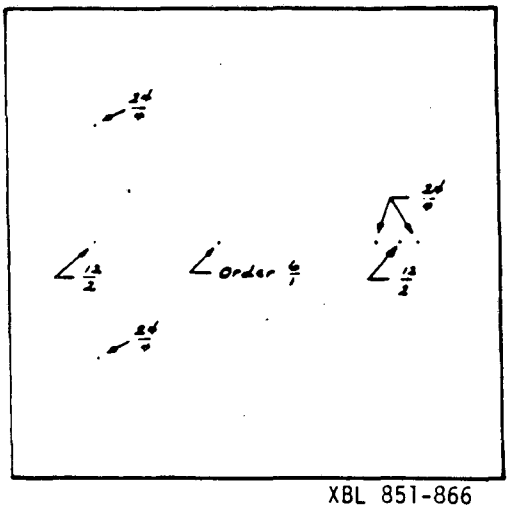

XBL 851-866

Fig. III.21 A = 0.2667

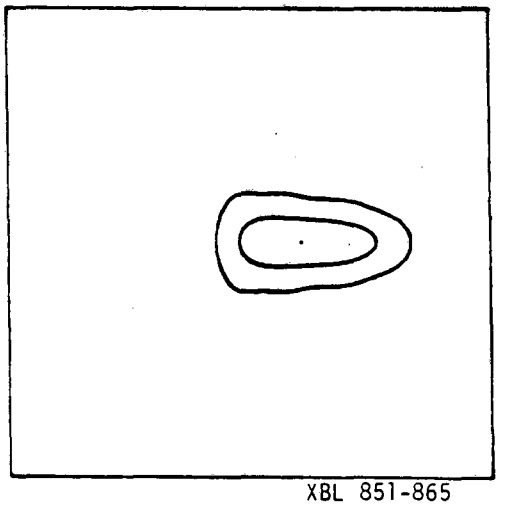

XBL 851-865

Fig. III.22 A = 0.2651
6th order fixed point is stable.

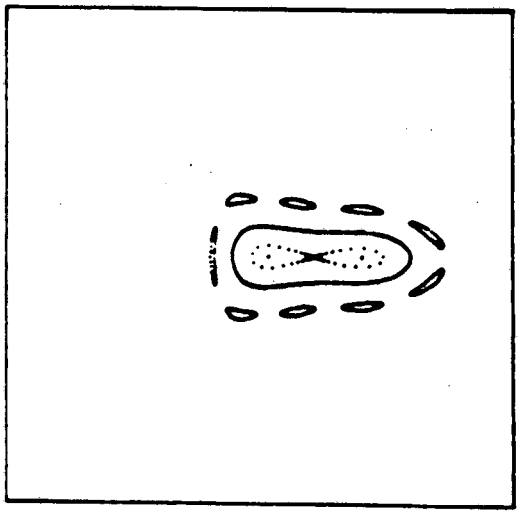

Fig. III.23 A = 0.2652
XBL 851-864

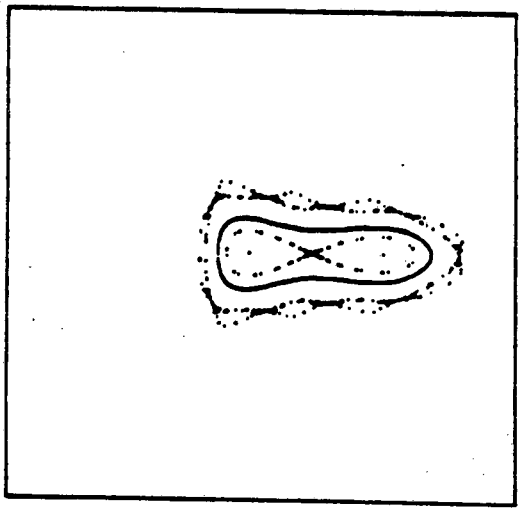

Fig. III.24 A = 0.2653
XBL 851-886

Somewhat more detail may be seen on Figs. III.25 and III.26, with the scales:

Horizontal: -2.9 to -2.5, for x; Vertical: -0.003 to 0.003, for x'.

Fig. III.25, for A = 0.26520, is similar to Fig. III.23 (to a somewhat enlarged scale), but also suggests the presence of members of an order - 96/16 fixed-point system at the outer edge of the plot.

Fig. III.26, for A = 0.26525, illustrates in somewhat greater detail features such as were evident (for A = 0.26520) on Fig. III.25. The strong scatter of points seen on the present figure results from a run launched substantially at one of the fixed points of the unstable order - 96/16 fixed-point system.

The bifurcation leading to an order - 24/4 system is illustrated by Figs. III.27 and III.28, to the scales:

Horizontal: -2.60 to -2.45, for x; Vertical: -0.0002 to 0.0002, for x'.

Fig. III.27 for A = 0.26663, shows an order - 12/2 fixed point (stable for this value of A) situated on the negative x' axis (at x ≡ -2.522870) and two surrounding phase trajectories.

Fig. III.28, for A = 0.26665, shows the order - 12/2 fixed point (now unstable, and situated at x_0 ≡ -2.521895) and the associated development through bifurcation of an order - 24/4 system of which two fixed points are shown.

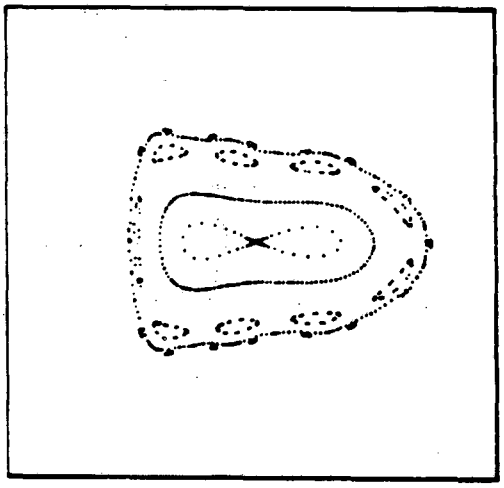

Fig. III.25 A = 0.2652
XBL 851-885

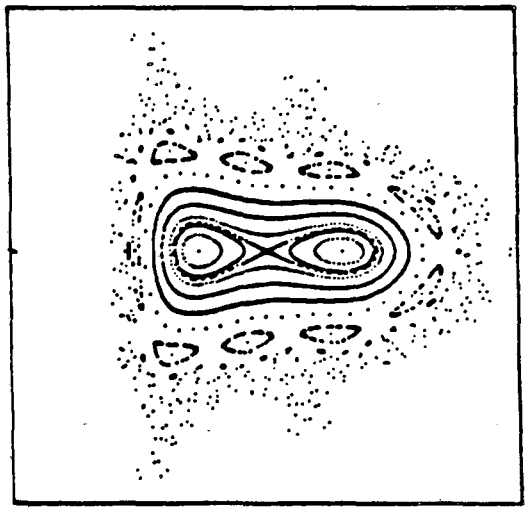

Fig. III.26 A = 0.26525
XBL 851-884

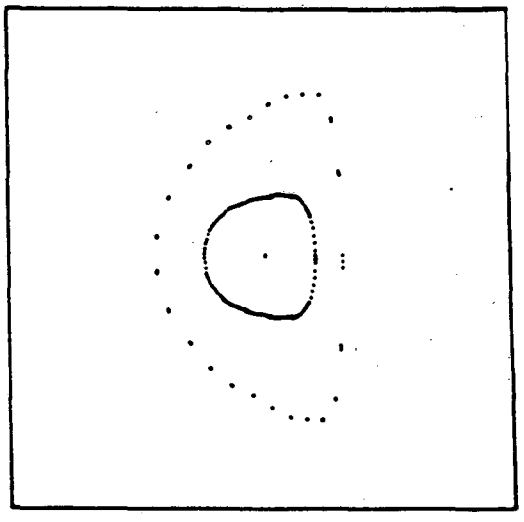

Fig. III.27 A = 0.26663
XBL 851-883

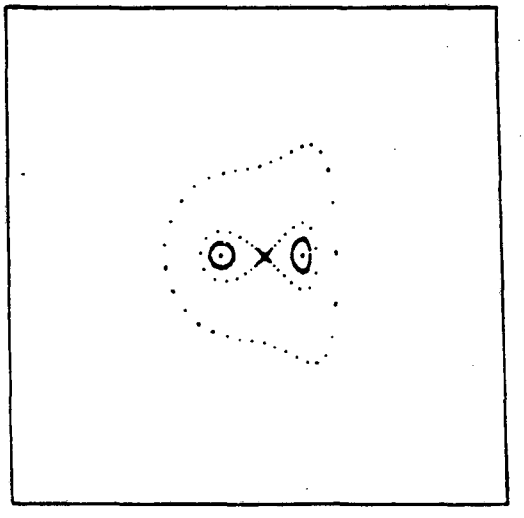

Fig. III.28 A = 0.26665
XBL 851-882

Figure III.29 shows the trend, vs. A, of the tangential-mapping half trace for the fixed-point systems just discussed. On sees, as the half trace of one system passes to values more negative than -1, the genesis of a new system of double period.

Figure III.30 indicates the development of a bifurcation tree that depicts, for fixed points situated on the negative x-axis, the locations (and hence the spacings) of the fixed points for the systems just discussed.

One also finds a fixed-point system of order 11/2 (σ = 2x360/11 = 65.4545...) from which, as the parameter A is increased, period-doubling bifurcations develop -- see Tables IV and V. The transition leading to the birth of an order - 22/4 system is illustrated by Figs. III.31 and III.32, to the scales:

Horizontal: 1.795 to 1.805, for x; Vertical: -0.01 to 0.01, for x'.

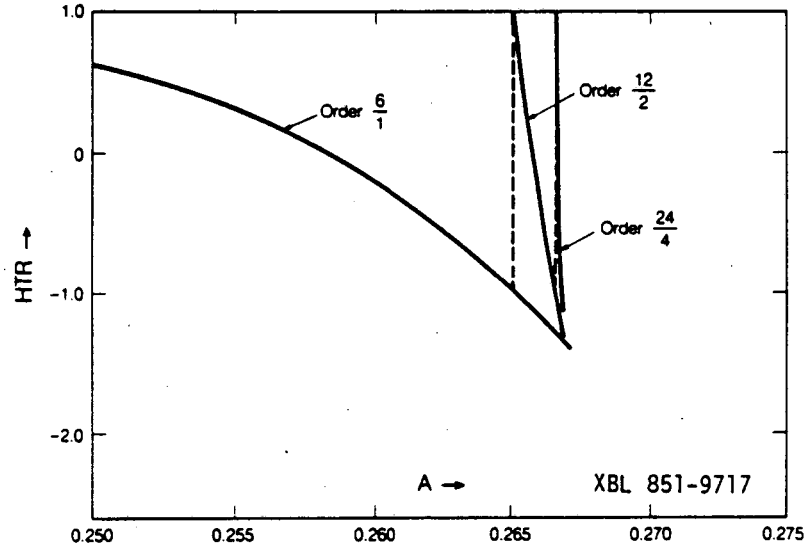

Fig. III.29

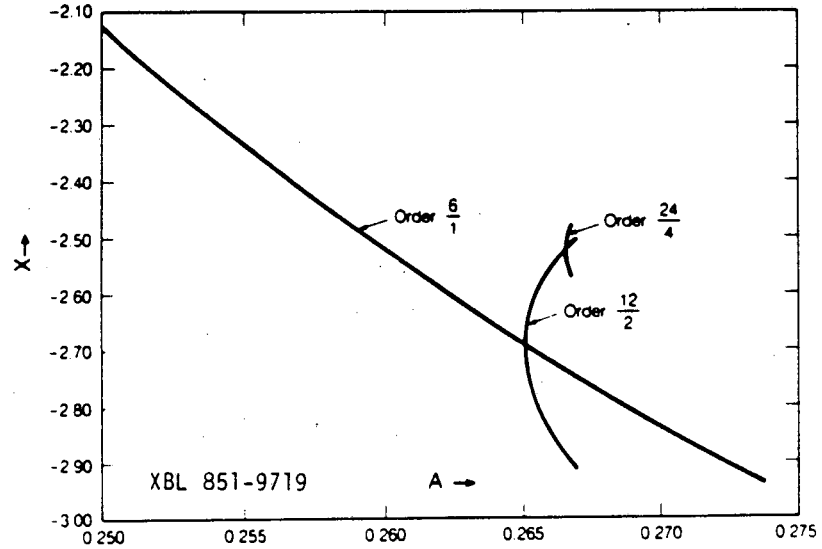

Fig. III.30

TABLE IV Coordinates on x-axis of Order -- 11/2 Fixed-Point Systems

A	Small-Amp'l Tune, σ_0 (Deg.)	HTR > +1		HTR < +1	
		x	HTR	x	HTR
0.2500	67.27394	-0.999353	1.000189	0.903246	0.999810
0.2550	68.79742	-1.347417	1.005812	1.193517	0.994174
0.2600	70.33441	-1.600037	1.050365	1.409902	0.949182
0.2650	71.88555	-1.786583	1.247550	1.581892	0.746606
0.2667	72.41629	-1.837753	1.391772	1.632457	0.595998
0.2668	72.44756	-1.840593	1.402071	1.635320	0.585177
0.2670	72.51013	-1.846219	1.423348	1.641007	0.562794
0.2675	72.66665	-1.859973	1.480681	1.655016	0.502310
0.2680	72.82332	-1.873297	1.544336	1.668729	0.434871
0.2700	73.45155	-1.922605	1.873355	1.720731	0.081897
0.2725	74.24035	-1.976496	2.500251	1.779691	-0.608400
0.2734	74.52529	-1.994150	2.800794	1.799374	-0.946613
0.2735	74.55698	-1.996062	2.837019	1.801512	-0.987672
0.27355	74.57283	-1.997014	2.855352	1.802578	-1.008476
0.2736	74.58868	-1.997964	2.873835	1.803641	-1.029466
0.2737	74.62039	-1.999857	2.911251	1.805761	-1.072004
0.2738	74.65210	-2.001741	2.949273	1.807871	-1.115298
0.2739	74.68382	-2.003615	2.987909	1.809971	-1.159359
0.2740	74.71554	-2.005481	3.027166	1.812062	-1.204199
0.27425	74.79488	-2.010106	3.128075	1.817249	-1.319776
0.2745	74.87426	-2.014678	3.233031	1.822377	-1.440468
0.2750	75.03314	-2.023668	3.455560	1.832462	-1.697941

TABLE V Some Coordinates of Order - 22/4 Systems

A	Small Amp'l Tune, σ_0 (Deg.)	x	$\pm x'$	HTR
0.27355	74.57283	1.801872	0.003584	0.932590
0.2736	74.58868	1.801200	0.006667	0.769102
0.2737	74.62039	1.799858	0.010374	0.452546
0.2738	74.65210	1.798516	0.013068	0.150275
0.2739	74.68382	1.797176	0.015292	-0.137238
0.2740	74.71554	1.795837	0.017231	-0.409504
0.2742	74.77901	1.793162	0.020564	-0.906304
0.27424	74.79171	1.792627	0.021167	-0.997749
0.27425	74.79488	1.792494	0.021315	-1.020187
0.2745	74.87426	1.789158	0.024729	-1.524411

Fig. III.31, for A = 0.27350, shows a stable order - 11/2 fixed point situated on the positive x-axis and surrounded by a small closed phase trajectory.

Fig. III.32, for A = 0.27360, shows the evolution of eigenvector directions extended from the order - 11/2 fixed point (now unstable, with reflection) situated on the positive x-axis. Small loops are seen to be generated in this way, within which one sees two fixed points (and surrounding curves) of a stable order - 22/4 system that has come into existence for this value of A.

Fig. III.33, again for A = 0.27360, presents information related to that of Fig. III.32, but to the somewhat more extended scale:

Horizontal: 1.1 to 1.9, for x; Vertical: -0.15 to 0.15, for x'.

One sees now <u>three</u> small loops of the type for which one was shown on Fig. III.32, save that now the width of the loops is scarcely noticeable on the present scale. Also shown are two order - 11/2 fixed points for which HTR > +1 (indicated by arrows) and an indication of the stochastic behavior that rapidly develops from a launch in such a region of the phase plane.

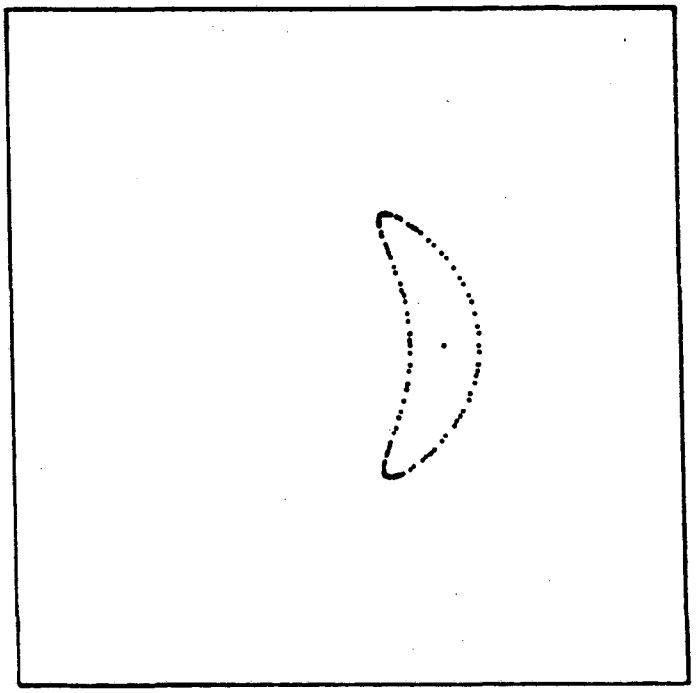

XBL 851-881

Fig. III.31 A = 0.27350

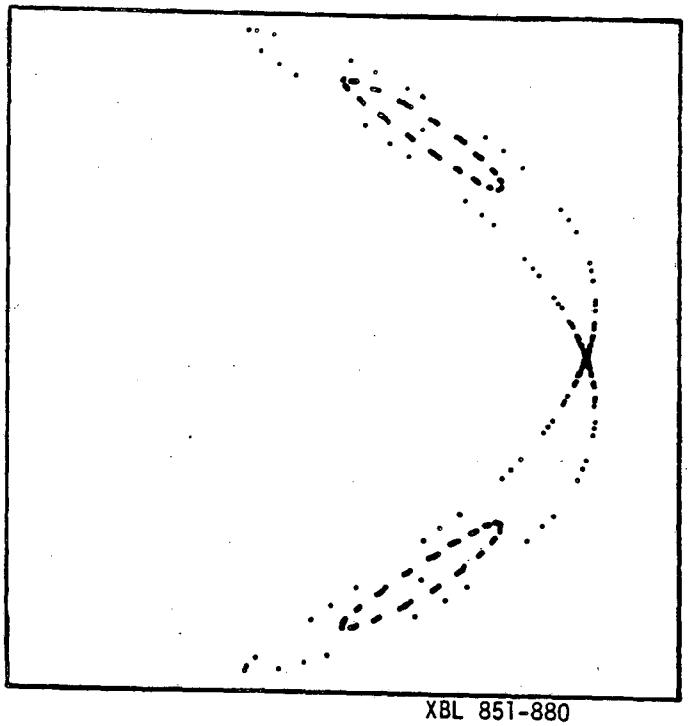

XBL 851-880

Fig. III.32 A = 0.27360

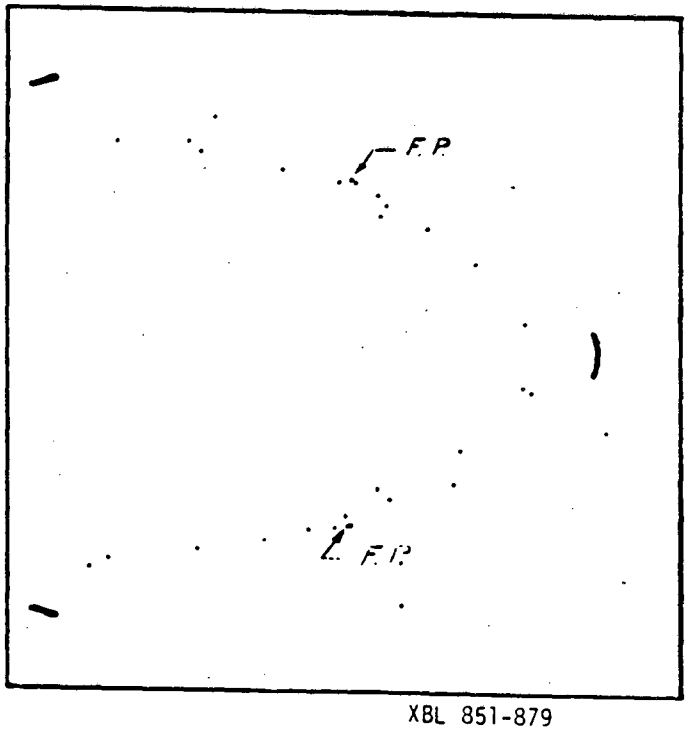

XBL 851-879

Fig. III.33 A = 0.27360

The fixed-point system of order 22/4 itself becomes unstable, with reflection, when the parameter A becomes as large as 0.27425 (as may be seen from Table V). The resulting additional bifurcation is illustrated on Fig. III.34 to the scales:

Horizontal: 1.785 to 1.800, for x; Vertical: 0.015 to 0.025, for x'.

Fig. III.34, for A = 0.27425, shows a narrow loop that develops from an extension of the eigenvector directions associated with the unstable order - 22/4 fixed point (unstable with reflection) situated near the center of the diagram. Such loops encircle stable fixed points of an order - 44/8 system, of which two are seen on the diagram (as indicated by arrows at, approximately,

$$x = 1.789457,\ x' = 0.022340$$

and

$$x = 1.795888,\ x' = 0.020075$$

The trend, vs. A, of HTR (the tangential-mapping half trace) for the order - 11/2 and order - 22/4 systems mentioned above is illustrated by the graph of Fig. III.35.

Additional fixed-point systems that lead to period-doubling bifurcation of course also can be found. We cite here, without further illustration, an order - 23/4 system that becomes unstable with reflection for A as great as 0.2628:

A	Small Amp'l Tune, σ_0 (Deg.)	Coordinate on Positive x axis	HTR
0.2627	71.17022	1.673937	-0.970413
0.2628	71.20126	1.675894	-1.057670

For A = 0.2628 an order - 46/8 stable system is formed (with HTR = 0.56173), for which one fixed point is found to be situated at

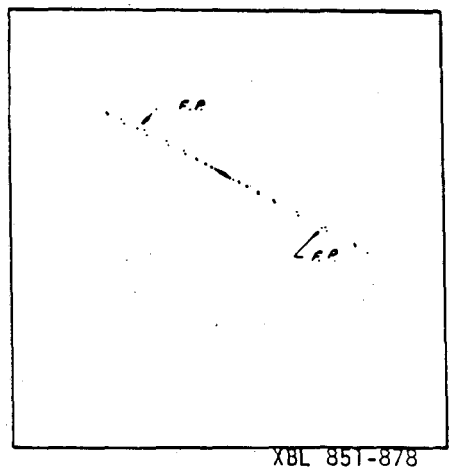

XBL 851-878

Fig. III.34 A = 0.27425

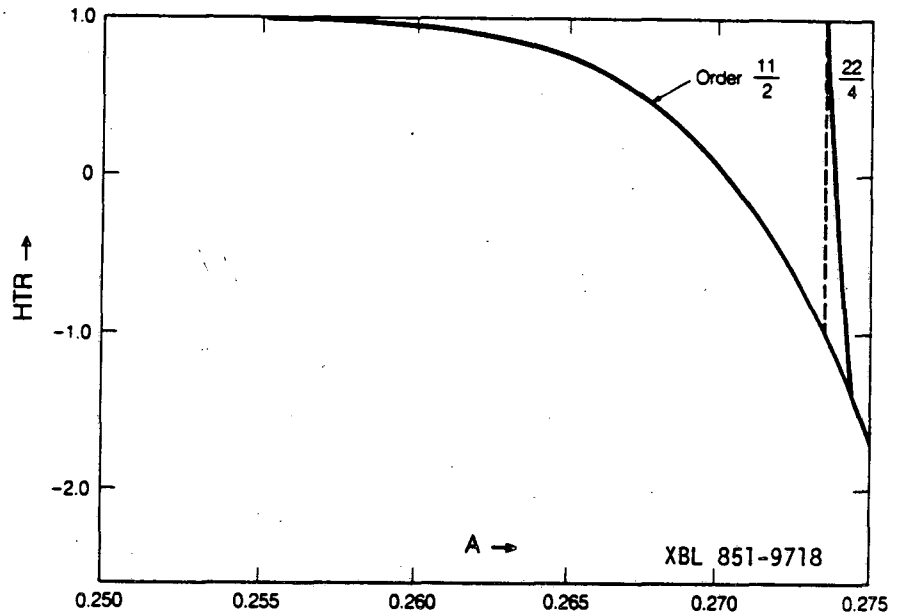

Fig. III.35

C. A Differential Equation with Cubic and Quintic Nonlinearity

The differential equation

$$\frac{d^2x}{dZ^2} + A\left(x + 1/12\, x^3 + 1/384\, x^5\right)\cos Z$$

also can be used to provide solutions that illustrate the occurrence of bifurcations. One sequence of examples can be introduced conveniently by considering two systems of order - 14/3 fixed-points for a range of values of the parameter A such that $0.200 \leq A \leq 0.2088$. One of these fixed-point systems will be strongly unstable for any value of A within the range mentioned, and for such a system two of the 14 fixed-points can be found to lie on the x-axis (at equal values of $|x|$). The other of these fixed-point systems is such that two members of any such system lie on the x'-axis (at equal values of $|x'|$) and will be locally stable for the larger values of A (such as A = 0.2087 and A = 0.2088). For values of A equal to 0.2086 or less, however , this second system also becomes locally unstable (HTR > +1) and one finds, as shall be illustrated, that additional fixed-point systems (at first, once again, only of order 14/3) then occur. Characteristics of the two order - 14/3 fixed-point systems mentioned earlier are listed in Table VI, wherein the columns headed HTR provide the half trace of the tangential-mapping transformation (for $\Delta Z = 14(2\pi)$). [For the second type of fixed-point system cited in Table VI, it is of interest to note that further increases of the parameter A carry the value of HTR to -1.0 (at A = 0.21619) but not beyond, since further increases of A then lead to HTR becoming less negative!]

TABLE VI Order -- 14/3 Systems

A	Small-Amp'l Tune, σ_0 (Deg.)	Fixed point at x'=0		Fixed point at x=0	
		±x	HTR	±x'	HTR
0.200	52.6619	2.132726	48.025758	0.242921	17.885314
0.201	52.9447	2.117613	42.423693	0.240836	14.320294
0.202	53.2278	2.102467	37.475516	0.238752	11.318874
0.203	53.5113	2.087283	33.107939	0.236670	8.806001
0.204	53.7951	2.072057	29.255340	0.234589	6.715351
0.205	54.0792	2.056788	25.859036	0.232509	4.988429
0.206	54.3637	2.041473	22.866618	0.230429	3.573762
0.2068	54.5915	2.029186	20.731897	0.228766	2.636284
0.2069	54.6200	2.027648	20.480026	0.228558	2.530064
0.207	54.6485	2.026109	20.231347	0.228350	2.426151
0.2075	54.7911	2.018409	19.034446	0.227310	1.939918
0.208	54.9337	2.010695	17.911591	0.226271	1.506006
0.2081	54.9623	2.009151	17.695506	0.226063	1.425130
0.2082	54.9908	2.007606	17.482168	0.225855	1.346147
0.2083	55.0194	2.006061	17.271542	0.225647	1.269025
0.2084	55.0479	2.004515	17.063595	0.225439	1.193734
0.2085	55.0765	2.002968	16.858294	0.225231	1.120243
0.2086	55.1050	2.001421	16.665604	0.225023	1.048520
0.2087	55.1336	1.999874	16.455495	0.224815	0.978538
0.2088	55.1621	1.998326	16.257932	0.224607	0.910265
0.209	55.2193	1.995228	15.870323	0.224192	0.778733
0.210	55.5052	1.979704	14.074649	0.222112	0.214188

A change in the character of phase-plane motion in the neighborhood of an order - 14/3 fixed-point is indicated on Figs. III.36-III.39 as a consequence of the system becoming unstable (HTR > +1) when the parameter A is reduced from A = 0.2087 to A = 0.2086. These plots are to the scales:

Horizontal: -0.001 to 0.001, for x; Vertical: 0.223 to 0.227, for x'.

Fig. III.36, for A = 0.2087, shows three small smooth phase trajectories encircling the stable order - 14/3 fixed point situated on the positive x' axis.

Fig. III.37, for A = 0.2086, shows a single loop that develops from a launch quite close to the now unstable order - 14/3 fixed-point situated on the x' axis at x' ≅ 0.225023. Because this fixed point has become unstable without reflection, it is possible for a single loop to be formed in this way.

Fig. III.38, again for A = 0.2086, shows the addition of an additional loop that arises from a separate run launched from the neighborhood of the unstable order - 14/3 fixed point. Each of these two loops encircles a fixed point of a new fixed-point system, but such fixed points constitute separate periodic orbits--and hence are members of separate new fixed-point systems, each of order 14/3 (no period-doubling).

Fig. III.39, again for A = 0.2086, shows further detail in the motion of phase points close to the unstable order - 14/3 fixed point and to the two new (stable) order - 14/3 fixed points present on this diagram.

The result of the change from A = 0.2087 to A = 0.2086 thus has been seen to involve the change of one order - 14/3 system from stable to unstable (HTR > +1) and the creation of two new stable systems of the same order. It is of interest now to follow the locations and stability characteristics of these new systems as the parameter A is further reduced. The fixed points of one of the new systems have phase-plane coordinates identical to coordinates of the other system, save for a reversal of sign for x'. Thus, for one of the stable fixed points shown on Fig. III.38 (for A = 0.2086) the coordinates are approximately

$$x = 0,\ x' = 0.226004$$

with a second member of this family at

$$x = 0,\ x' = -0.223995,$$

while for the other stable family fixed points occur at

$$x = 0,\ x' = 0.223995$$

and, for a second member of this family at

$$x = 0,\ x' = -0.226004$$

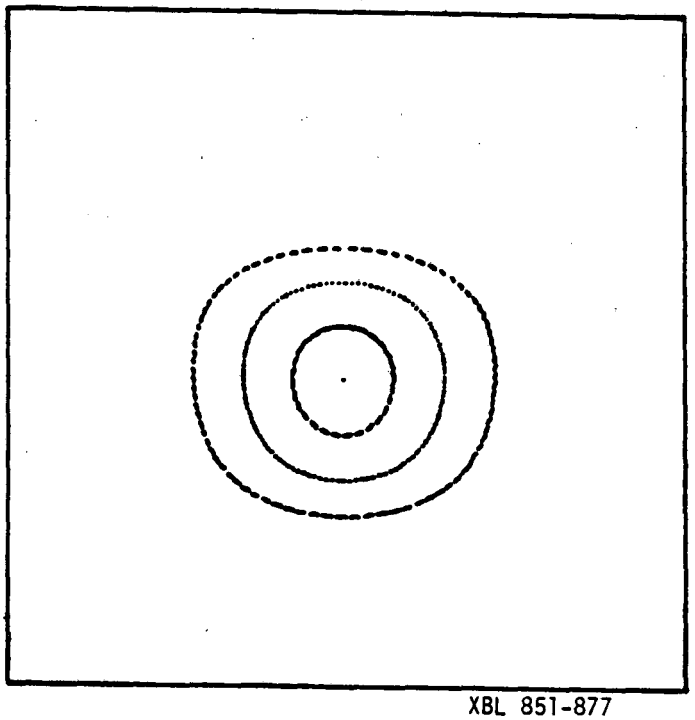

XBL 851-877

Fig. III.36 A = 0.2087, with cubic and quintic nonlinearity.
Scales: -0.001 to 0.001; 0.223 to 0.227.

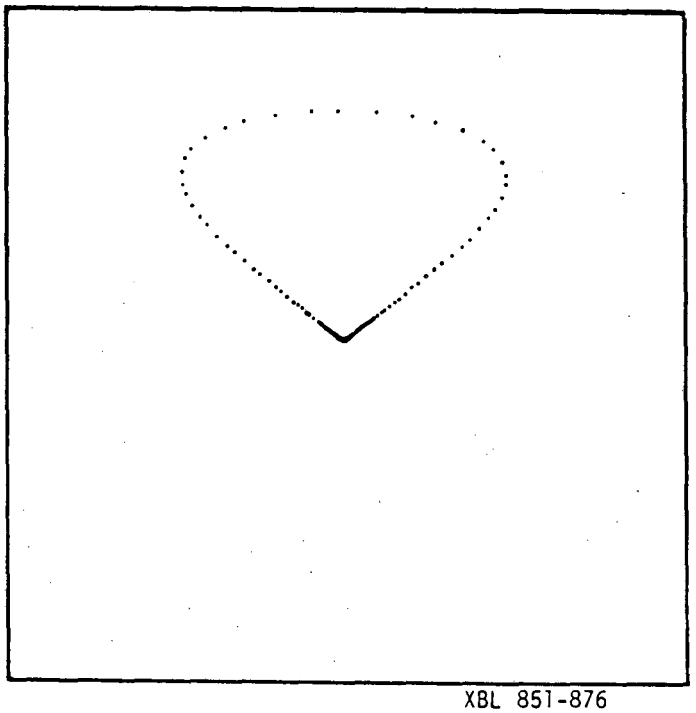

XBL 851-876

Fig. III.37 A = 0.2086, with cubic and quintic nonlinearity.
Scales: -0.001 to 0.001; 0.223 to 0.227.

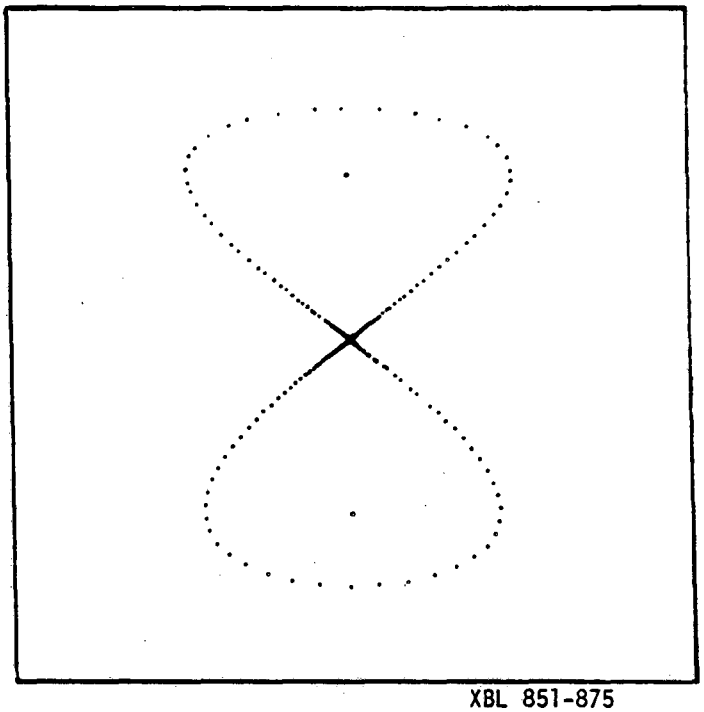

XBL 851-875

Fig. III.38 A = 0.2086, with cubic and quintic nonlinearity.
Scales: -0.001 to 0.001; 0.223 to 0.227.

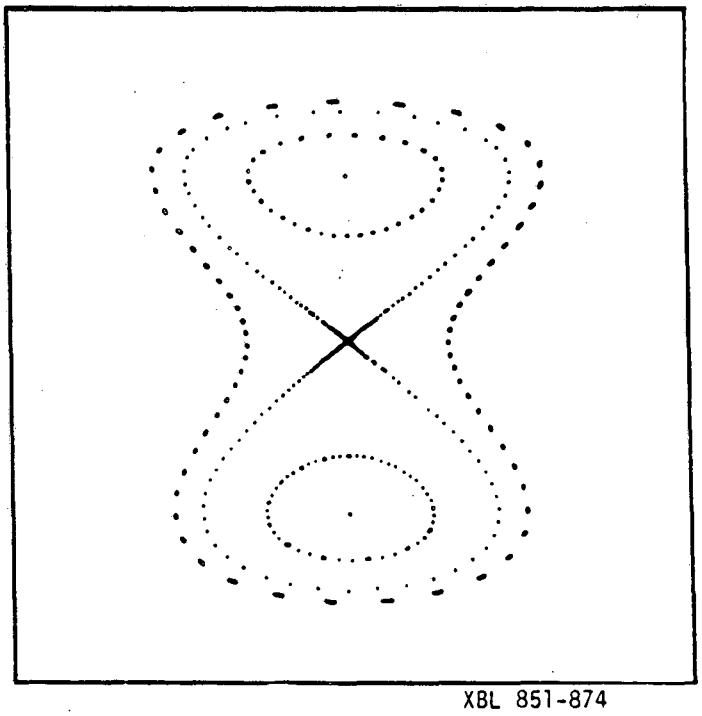

XBL 851-874

Fig. III.39 A = 0.2086, with cubic and quintic nonlinearity.
Scales: -0.001 to 0.001; 0.223 to 0.227

The locations of such fixed points on the positive x' axis are plotted, vs. A, on Fig. III.40 (together with similar information for one of the systems presented in Table VI). Table VII lists these x' values for the new order - 14/3 system, together with the associated value of the half trace (HTR) for the tangential-mapping transformation. It is seen from this tabulation that with reductions of the parameter A to 0.2069, and beyond, the value of HTR for these systems becomes less than -1. Associated with this transition into instability with reflection one may now expect to find (as will be illustrated) the occurrence of period-doubling bifurcation.

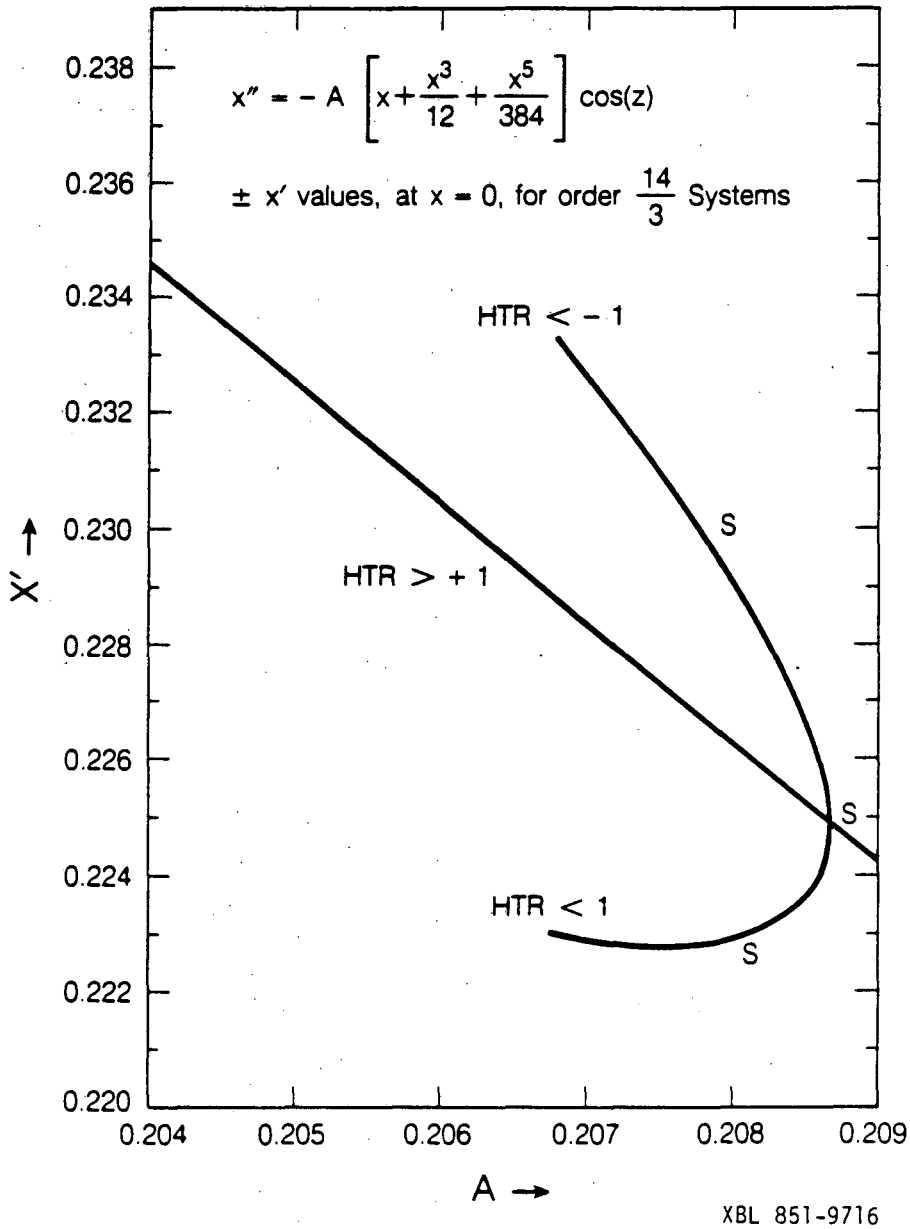

XBL 851-9716

Fig. III.40

TABLE VII Additional Order - 14/3 Fixed Points on x'-Axis

A	Small Amp'l Tune, σ_0 (Deg.)	$\pm x'$	$\bar{+}x'$	HTR
0.2068	54.5915	0.233266	0.222992	-1.090469
0.2069	54.6200	0.232957	0.222952	-1.007070
0.2070	54.6485	0.232643	0.222916	-0.920183
0.2075	54.7911	0.230997	0.222818	-0.435180
0.2080	54.9337	0.229147	0.222930	0.129613
0.2085	55.0765	0.226742	0.223602	0.768309
0.2086	55.1050	0.226004	0.223995	0.904419

Figures III.41 and III.42, for A = 0.2070, respectively indicate the phase motion about the fixed points that Table VII shows to be situated on the x' axis at x' ≅ 0.232643 and at x' ≅ 0.222916 -- plotted to the scales:

For Fig. III.41 Horizontal: -0.004 to 0.004, for x;

Vertical: 0.2326 to 0.2327, for x'.

For Fig. III.42 Horizontal: -0.0005 to 0.0005, for x;

Vertical: 0.22235 to 0.22345, for x'.

For A = 0.2069, the fixed points shown on Figs. III.41 and III.42 have become unstable with reflection, and are situated on the x' axis at the respective locations x' ≅ 0.232957 and x' ≅ 0.222952. The extension of eigenvector directions from such fixed points then indicates that each has given rise to an order - 28/6 fixed-point system (period-doubling bifurcation). The stable order - 28/6 fixed points close to x = 0, x' = 0.232957, are found to lie at x ≅ ± 0.001123, x' ≅ 0.232949, as indicated on Figs. III.43 and III.44 to the scales:

Horizontal: -0.004 to 0.004, for x;

Vertical: 0.2329 to 0.2330, for x'.

The stable order - 28/6 fixed points close to x= 0, x' ≅ 0.222952 are found to lie on the x'-axis at x' ≅ 0.223175 and x' ≅ 0.222750 (constituting a second stable system of order 28/6), as can be seen on Figs. III.45 and III.46 to the scales:

Horizontal: -0.0001 to 0.0001, for x;

Vertical: 0.2224 to 0.2235, for x'.

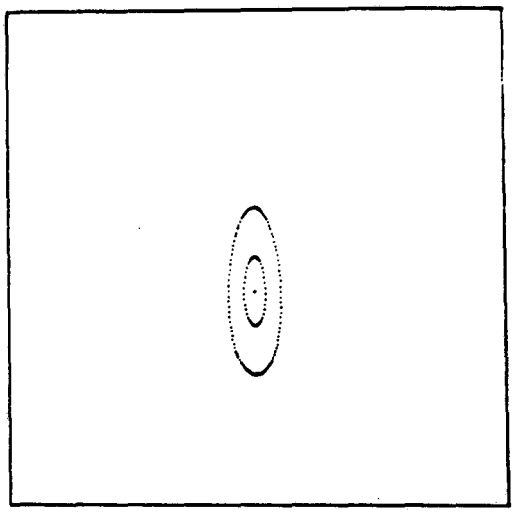

XBL 851-873

Fig. III.41 A = 0.2070,
with cubic and quintic nonlinearity.

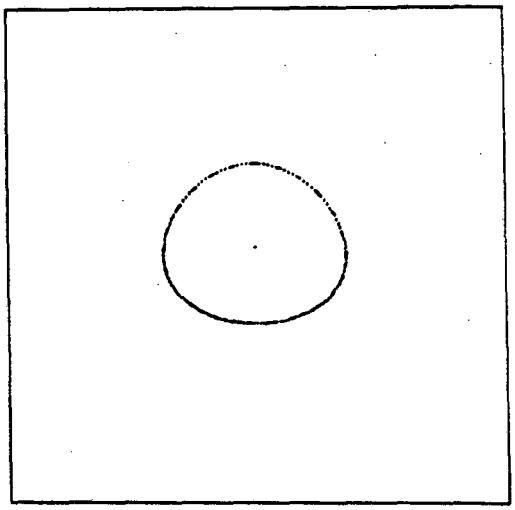

XBL 851-872

Fig. III.42 A = 0.2070,
with cubic and quintic nonlinearity.

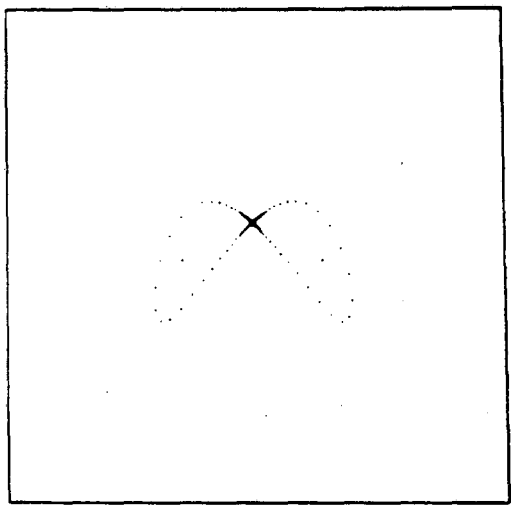

XBL 851-871

Fig. III.43 A = 0.2069,
with cubic and quintic nonlinearity.

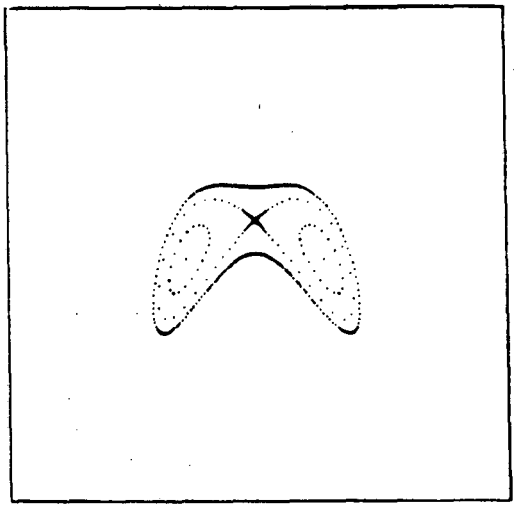

XBL 851-870

Fig. III.44 A = 0.2069,
with cubic and quintic nonlinearity.

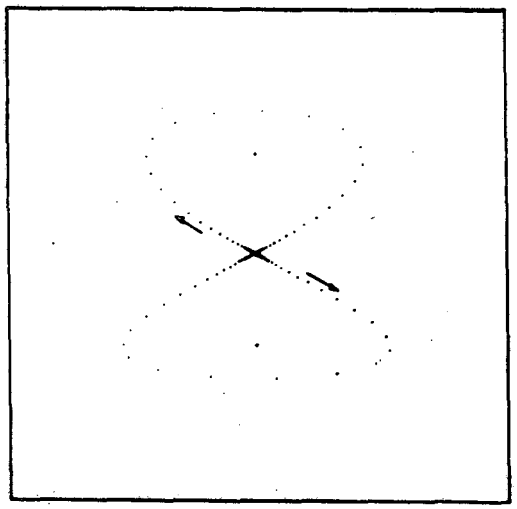

XBL 851-869

Fig. III.45 A = 0.2069,
with cubic and quintic nonlinearity.

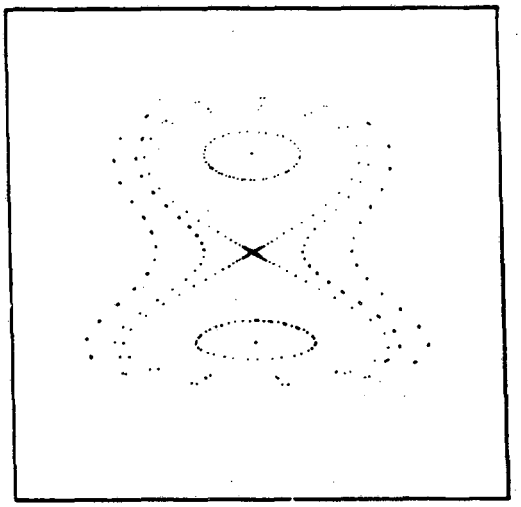

XBL 851-868

Fig. III.46 A = 0.2069,
with cubic and quintic nonlinearity.

REFERENCES OR NOTES

1. Computational illustrations of period-doubling bifurcations have been given in a paper by T. C. Bountis, "Period Doubling Bifurcations and Universality in Conservative Systems," Physica D, 3D, No. 3, 577-589 (August, 1981).

2. The tangential-mapping transformation about the fixed points (x_n, y_n) of M^N is represented by the matrix product

$$\prod_{n=1}^{N} \begin{pmatrix} F'(x_n) & 1 \\ -1 + F'(x_n)\,F'(x_{n+1}) & F'(x_{n+1}) \end{pmatrix} .$$

LAWRENCE BERKELEY LABORATORY
TECHNICAL INFORMATION DEPARTMENT
UNIVERSITY OF CALIFORNIA
BERKELEY, CALIFORNIA 94720